AN EXPERIMENTAL STUDY OF NEAR WAKE STRUCTURE BEHIND LINEARLY TAPERED CYLINDERS

by

Sanjay Kumar

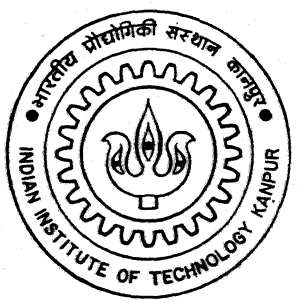

DEPARTMENT OF AEROSPACE ENGINEERING

INDIAN INSTITUTE OF TECHNOLOGY KANPUR

APRIL, 1996

AN EXPERIMENTAL STUDY OF NEAR WAKE STRUCTURE BEHIND LINEARLY TAPERED CYLINDERS

A thesis submitted in partial fulfillment of the
requirements for the degree of

MASTER OF TECHNOLOGY
in
AEROSPACE ENGINEERING

by

SANJAY KUMAR

to the

Department of Aerospace Engineering
Indian Institute of Technology
Kanpur 208016
India

April 1996

SAV

AE-1996-M-~~KSM~~-EXP

DEDICATED

to

MY PARENTS

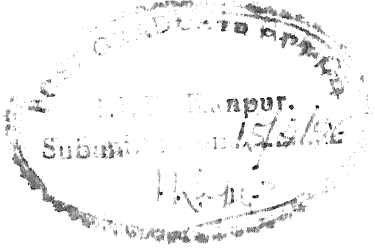

CERTIFICATE

It is certified that the work presented in this thesis entitled " **An experimental study of near wake structure behind linearly tapered cylinders**" has been carried out under my supervision in partial fulfillment of the requirements for the award of M.Tech degree in Aerospace Engineering. This thesis is a record of bonafied work carried out in the Dept. of Aerospace Engineering, I.I.T. Kanpur during the year 1995 - 96 and this work has not been submitted elsewhere for a degree.

Dr K. Poddar
Professor
Department of Aerospace Engineering
Indian Institute of Technology
Kanpur

April 1996

ACKNOWLEDGEMENTS

I would like to place on record my gratitude to my advisor Dr K. Poddar, Professor, Department of Aerospace Engineering, I.I.T, Kanpur. His encouraging attitude has been of immense help during the M.Tech program.

I am also thankful to Mr. Rameshwar, Mr. H.C. Bhattacharya, and Mr. K. Mohan for their help in fabricating models and in setting up the experiments.

My special thanks to Rishi Raj Pandey, Akhilesh Raghuvanshi and Manish Jain who combined to make life at I.I.T Kanpur enjoyable. My greatest debt is to my parents.

April 1996

Sanjay Kumar
Department of Aerospace Engineering
Indian Institute of Technology
Kanpur

TABLE OF CONTENTS

LIST OF FIGURES

FIGURE 13. Flow visualization pictures for models with taper ratios of a) 60 : 1, b) 80 : 1, c) 120 : 1, and d) 180 : 1. In all the pictures the flow direction is from left to right. Arrows indicate the locations of vortex splitting.

FIGURE 14. Oblique vortex shedding behind straight cylinder without any control cylinder. a) Flow visualization b) Base pressure distribution.

FIGURE 15. Vortex shedding geometry and base pressure distribution with control cylinder($D/d = 3$) at $Z/d = 69$ and $X/d = 9.3$.

FIGURE 16. Parallel shedding induced by a control cylinder($D/d = 3$) at optimal location of $Z/d = 69$ and $X/d = 6$. a) Flow visualization b) Base pressure distribution.

FIGURE 17. Vortex shedding geometry and base pressure distribution with control cylinder($D/d = 3$) at $Z/d = 69$ and $X/d = 4.1$.

FIGURE 18. Variation of 'control cylinder location for inducing parallel shedding' along the span for various control cylinder diameters. $\triangle$, $D/d = 4$; $\bigcirc$, $D/d = 3$; $\diamond$, $D/d = 2.5$.

FIGURE 19. Vortex shedding geometry and base pressure distribution on tapered cylinder of taper ratio 150 at $Re_{cs} = 80$.

FIGURE 20. Vortex shedding geometry and base pressure distribution on tapered cylinder of taper ratio 150 at $Re_{cs} = 120$.

FIGURE 21. Vortex shedding geometry and base pressure distribution on tapered cylinder of taper ratio 150 at $Re_{cs} = 150$.

FIGURE 22. Control cylinder technique applied to tapered cylinder of taper ratio 150 : 1 at $Re_{cs} = 120$. a) Vortex shedding geometry without control cylinder b) Vortex shedding geometry with control cylinder. Arrow shows the location of control cylinder.

NOMENCLATURE

d	Test cylinder diameter.
d_1	Smaller of the two end diameters of tapered cylinder.
d_2	Greater of the two end diameters of tapered cylinder.
d_m	Centerspan diameter of tapered cylinder.
f	Shedding frequency in Hertz.
l	Length of tapered cylinder.
C_p	Pressure coefficient, $(P_b - P_\infty)/\frac{1}{2}\rho U_\infty^2$.
D	Control cylinder diameter.
P_b	Base pressure.
P_∞	Free stream static pressure.
Re	Reynolds number.
Re_{cs}	Reynolds number based on centerspan diameter of tapered cylinder.
R_T	Taper ratio, $1/(d_2\text{-}d_1)$.
St	Strouhal number.
U_∞	Free stream velocity.
X,Y,Z	Axes convention.
ρ	Free stream density.

ABSTRACT

The near wake structure behind linearly tapered cylinders has been studied in the present investigation. Four tapered cylinders with taper ratios of 60:1, 80:1, 120:1 and 180:1 were examined at Reynolds numbers 80, 120 and 146 (based on centerspan diameter). It was observed that there exist discrete shedding cells with constant frequency across the span, frequency being different in each cell. The number of cells and the cell lengths, for each of the four cylinders, were measured at the three Reynolds numbers. Measurements indicate that at a fixed Reynolds number the number of cells first decrease with increasing taper ratio and then reach an asymptotic value. It was also observed that the number of cells increased with increasing Reynolds number. Visualization study provided detailed structure of the shedding vortices. Vortex splitting was evident at the boundary of two cells; and it was found to occur in more spanwise locations with decreasing taper ratio indicating formation of more cells.

Control of the wake geometry was first achieved for straight cylinder and the same technique was tried to control the wake geometry of tapered cylinders. A control technique of placing a vertical control cylinder towards one end of the straight test cylinder to control the shedding geometry (by manipulating the base pressure distribution) at fixed Reynolds number and oblique angle is developed. Three control cylinders of different diameters were tried. An experimental graph is obtained to predict the location of control cylinder of given diameter to obtain parallel shedding. Base pressure measurements were made for both oblique and parallel shedding. Measurements revealed that base pressure was constant over the region where the shedding was parallel.

The same technique was tried to control the wake geometry (obliqueness) behind tapered cylinder of taper ratio 150. Visualization study shows that the technique developed indeed works for tapered cylinder near the region of control cylinder location.

Vortex shedding behind bluff bodies has been an extensive research topic for a long time. Past studies in this area were mostly confined to bluff bodies of spanwise uniform cross section. In particular, the classical phenomenon of vortex shedding from straight cylinders with no generic three-dimensional effects has been studied in some detail and various flow regimes have been classified. Roshko [1] carried out an extensive low Reynolds number investigation of vortex shedding from straight cylinders. He found that very regular shedding took place over a Reynolds number range of about 47 - 170; above this upper limit the process became irregular and the frequency difficult to define. He used hot wire probes in the wake to obtain shedding frequencies within the regular range and found that these followed the empirical law

$$St = 0.212 - 4.5/Re,$$

where $St = fd/U_\infty$ and Re is based on test cylinder diameter.

However, very little attention had been paid to study the influence of slight three dimensionality in the model, e.g. taper. This thesis describes the effects of taper on near wake structure of linearly tapered cylinders. Such effects are important in the study of vortex shedding behind bluff bodies.

1.1 Literature Survey

The study of vortex shedding behind a linearly tapered cylinder was first reported by Gaster [2]. He investigated flow past two tapered cylinders in a water tunnel with taper ratios of 36:1 and 18:1. He discovered that the fluctuating velocity signal was modulated consisting of two distinct frequencies in the wake of the tapered cylinder. The modulated signal appeared at all spanwise locations behind both of his cylinders, at all Reynolds numbers between 66 and 172. He suggested that vortices are shed in

patches with predominant frequency in the patch varying continuously along the span of the cylinder while modulation frequency remaining constant.

In a later study, Gaster [3] investigated the flow behind a mildly tapered cylinder of taper ratio 120:1 in a wind tunnel. He found that the vortex wake structure exists in a number of discrete cells having different shedding frequencies. Within each cell shedding is regular and periodic, the frequency being somewhat lower than from a parallel cylinder of the same diameter. He also observed similar type of wake behaviour on a parallel model in a non uniform mean flow. These results confirmed his earlier results.

Recently, Van Atta and Piccirillo [4] also observed cellular structures behind cylinders with taper ratios of 13 : 1, 23 : 1 and 32 : 1. They also found that the difference in shedding frequencies between two adjacent cells was a constant. They concluded from their study that vortex splitting was the mechanism which connects two adjacent cells. The vortex splitting phenomenon was also seen by Lewis and Gharib [5] in the wake of a cylinder with discontinuity in diameter.

Noak, Ohle and Eckelmann [6] examined the problem theoretically by proposing a simple phenomenological model of non linearly coupled Van der pol oscillators for the formation of spanwise cells behind slender bodies of revolution in crosswise, uniform or non uniform oncoming flow. The model yields all qualitative features found in experiments, including the formation of cells, a reduced amplitude of oscillation due to the coupling, discrete power spectra, non linear beat near the cell boundaries, slanted vortex shedding within a cell, and the presence of vortex splitting. They compared the results with their experiments on 90:1 taper ratio cylinder. Their theoretical results qualitatively agreed with the experimental results but an accurate estimate of shedding frequencies could not be obtained. So further improvements on the model are needed. Similar results were obtained by Gerich and Eckelmann [7], who found that the straight

cylinder end boundaries, whether they be end plates or simple free ends, alter the vortex shedding mechanism near these boundaries. They found that in a region near an end plate or a free end (ranging from 6 to 15 cylinder diameters in length), the shedding frequency is 10 - 15% less than the regular Strouhal frequency. The latter frequency is observed over the remaining cylinder length. The simultaneous occurrence of two frequencies results in a beat frequency, which is best observed at the junction of the two regions. A third frequency is observed over the entire cylinder length when the cylinder is bounded by two end plates less than 20 to 30 cylinder diameters apart.

More recently, Piccirillo and Van Atta [8] studied flow behind tapered cylinders with taper ratios varying from 50:1 to 100:1. They confirmed that the flow consist of discrete shedding cells, each with a constant frequency. For a centerspan Reynolds number greater than 100, the dimensionless mean cell length was found to be constant. Individual cell size was found to be roughly self similar. New shedding cells were created at the ends of the cylinders, or in the region adjacent to the area where there is no shedding. Successful scalings were found for both the shedding frequency of the cells and their differences. The modulation frequencies were found to be constant along the cylinder span. The Strouhal number - Reynolds number curve was found to have a slightly steeper slope than the Strouhal number curve for a non tapered cylinder. The primary effect of the taper was to introduce vortex splits which form the links between shedding cells. These vortex splits begin with a kink which deepens and moves towards the narrow end of the cylinder.

The experiments on tapered cylinders were confined to the study of wake structure. No information is available in the published literature for controlling the wake geometry behind tapered cylinders. However, extensive study has been done for controlling the wake geometry behind straight circular cylinders.

Past experiments on wakes of straight circular cylinders in a laminar flow have

shown that the vortex shedding is two dimensional only at low Reynolds numbers. As a certain transition Reynolds number is reached the vortex shedding becomes oblique, where the vortices are parallel to each other but inclined with respect to the cylinder axis. Tritton [9] found a discontinuity in the velocity - frequency curve. This discontinuity occurred at $Re = 90$ in wind tunnel experiments and $Re = 70$ in water tunnel experiments. He did not link the appearance of the discontinuity to possible changes of the geometry of the shed vortices, but interpreted it instead as a transition in the nature of the flow instability from a vortex street originating in the wake to the vortex street originating in the immediate vicinity of the cylinder. Tritton's interpretation was disputed by several authors who were of the opinion that it was solely due to end effects or flow induced vibrations or shear in the mean flow. A study of the effect of the geometry at the cylinder ends on the angle and frequency of vortex shedding was conducted by Ramberg [10] who measured vortex shedding frequency , the shedding angle, the base pressure, the vortex formation region length and wake width for stationary yawed circular cylinder in the Reynolds number range of 150 - 1100. He performed the experiments for free ended cylinder and cylinder fitted with end plates. An intrinsic interdependence between the shedding frequency and the shedding angle was observed and was used to determine, from simple discharge vorticity considerations, the type(s) of end conditions appropriate to the simulation of an infinitely long cylinder.

Williamson [11] showed that end plates suitably angled with respect to the incoming flow can be used to induce parallel vortex shedding resulting in completely continuous Strouhal curve which agrees very well with the oblique shedding data. This gave an indication that the Strouhal curve is universal (for a straight circular cylinder). Eisenlohr and Eckelmann [12] used end plates combined with larger diameter cylinders inserted at the ends of the main cylinder to control the wake geometry. They found that a "design break line" of vortex axes can lead to the decoupling of a wake flow from the ever present disturbances deriving from the ends and this decoupling gives rise to par-

allel vortex shedding. Hammache and Gharib [13] showed that oblique vortex shedding is solely due to geometrical flow conditions at the ends of the cylinder. They created a control technique (called transverse cylinder control technique, TCCT by them) to create vortex shedding of different geometries. In this technique two transverse circular cylinders were positioned upstream of the main shedding cylinder to control the angle of shedding from the main cylinder. The respective distances between each transverse cylinder and the main cylinder were used to induce vortex shedding of different geometries, including parallel shedding. Measurements of the mean static pressure distribution in the base region of the cylinder and of the mean spanwise component of the velocity in the wake were taken. These measurements revealed that a non symmetric pressure distribution, which induced a spanwise flow in the base region of the cylinder, was responsible for the oblique shedding. Parallel vortex shedding showed a symmetric pressure distribution with zero spanwise component of the velocity and zero cross - shear in the cylinder base. He also showed that the parallel vortex shedding results in a continuous Strouhal - Reynolds number curve.

1.2 Present Investigation

The flow behind three-dimensional bluff bodies of which tapered cylinder is the simplest example, is not yet clearly understood. There are many questions which remain to be answered, e.g. what happens at the boundary of the cells? Is the cell boundary a sharp one or fairly broad? Does the boundary shift in time? How do the cells interact with each other? What is the exact nature of vortex splitting? What is the effect of Reynolds number on the cellular structures? Can we control the wake geometry behind tapered cylinders?

Keeping these questions in mind an experimental investigation was carried out first to study the near wake flow behind linearly tapered cylinders with the help of

both flow visualization and quantitative measurements and then the control of wake geometry behind tapered cylinders is attempted through a technique developed for the straight cylinders. In the present investigation the aim was to address the question on the number of cells, the nature of boundary between two cells and the effect of Reynolds number. The experiments were carried out on four tapered cylinders with taper ratios of 60:1, 80:1, 120:1, and 180:1 at centerspan Reynolds numbers 80, 120 and 146. Flow visualization was done to visualize the structure of the shedding vortices and to correlate them with the quantitative measurements. Flow visualization on a straight cylinder (with no taper) was also done to compare the vortex shedding geometry with the tapered cylinder case.

In an attempt to control the wake geometry behind tapered cylinders, the control of wake geometry(obliqueness of shed vortices) was first attempted on straight cylinders where the flow field is simpler. The knowledge thus gained is used to control the wake geometry behind a tapered cylinder. The recent studies [13] showed that it is the end conditions which are responsible for various shedding geometries and by manipulating the condition at one end parallel shedding can be induced. So one transverse control cylinder was placed near the end plate to alter the end conditions and control the wake geometry as opposed to Hammache and Gharib [13] who used two control cylinders at two ends of the test cylinder. Firstly, oblique shedding was created by giving slight angle of attack to the end plate then this technique was employed to control its geometry (obliqueness). Mean base pressure was measured for different wake structure geometry. The experiments were carried out on a $2\,mm$ diameter cylinder at Reynolds number of 56. This value of Reynolds number ensured good flow visualization. Smoke wire technique proved to be very effective for flow visualization.

The same technique was then applied to control the wake geometry behind tapered cylinder of taper ratio 150:1. Base pressure measurements were done behind the tapered cylinder to correlate the results with the straight cylinder measurements.

2. EXPERIMENTAL PROGRAM

2.1 Facility

The experiments were carried out in the low speed low turbulence wind tunnel in the Aerodynamics Laboratory of Aerospace Engineering department at I.I.T Kanpur. It has test section dimension of $30\,cm \times 40\,cm \times 106\,cm$, contraction ratio of 9, a maximum wind speed of about $15\,m/sec$ continuously variable down to zero wind speed. A 2 h.p D.C motor drives an axial fan of about 45.7 cm diameter. The turbulence level of the tunnel is about 0.2% at the maximum wind speed. The experiments were, however, conducted at much lower wind speeds near $0.45\,m/sec$ at which the turbulence level of the tunnel was less than 0.06 %. The layout of the tunnel is shown in figure 1.

2.2 Model Geometry and Mounting System

The models consist of four tapered cylinders of taper ratios 60:1, 80:1, 120:1, and 180:1. All the cylinders had the same midspan diameter of $4\,mm$ and length $150\,mm$. The two ends of the models were so chosen that the same mounting system could be used for all the cylinders. A typical sketch of the tapered cylinder is shown in figure 2. The base pressure measurements on tapered cylinder were done on a hollow tapered cylinder of taper ratio 150:1 with centerspan diameter of $5\,mm$ and ten holes of diameter $0.8\,mm$ equally spaced on the surface to act as pressure taps. The same measurements on a straight cylinder were done on a $2\,mm$ diameter hollow stainless steel tube of roughly $1\,m$ length and a $0.6\,mm$ hole at the center to act as pressure tap. Three straight rods of diameters $5\,mm$, $6\,mm$ and $8\,mm$ were used as control cylinders.

The mounting system consists of two L-shaped aluminium stands of approximately airfoil cross section. The tapered cylindrical models with end plates of diameter $4\,cm$

were mounted at a height of 16 cm from the tunnel floor on these stands. The dimensions of the end plates were similar to those used by earlier researchers. A sketch of the model mounting system is shown in figure 3. A similar mounting system was used for straight cylinder except that the cylinder was also passed through the the tunnel side walls so that it could be pushed in and out of the tunnel to change the pressure port location. One end of the cylinder was blocked. A sketch of the model mounting system along with the model, instruments and axes convention is shown in figure 4 .

2.3 Instrumentation

The measurement of both mean and fluctuating components of the streamwise velocities were carried out in the wake. The free stream velocity was monitored with the help of a Pitot static tube placed in the free stream from the side of the tunnel; and it was connected to FC012 electronic micro-manometer manufactured by Furness controls ltd., Bexhill, England. The fluctuating u-component of the velocity was measured using a single hot-wire probe operated at constant temperature mode. An overheat ratio of 1.4 was applied to the hot-wire to keep the sensor at a higher temperature relative to the ambient fluid temperature. The signal from the hot wire probe was collected and analyzed by using an HP-35660A dynamic signal analyzer. The collected data records were 4 sec long and were sampled at a rate of 256 Hz, giving 1024 data points in each record for spectrum computation. To measure the cylinder base pressure, the open end of the cylindrical tube was connected to one of the ports of electronic manometer. To the other port was connected the static pressure of free stream. Thus the quantity that was monitored was $P_b - P_\infty$. It may be pointed out here that the experiments are very sensitive to small voltage fluctuations and very small gusts of air. Care was taken to avoid such disturbances.

2.4 Flow Visualization Technique

For flow visualization, smoke-wire technique was used, which proved to be very effective, and vortex shedding patterns were observed. A thin nichrome wire of diameter $0.015\,cm$ was passed through the end plates $2d_m$ behind the tapered cylinder and $2D$ behind the straight cylinder, where d_m is the centerspan diameter, and offset $1d_m$ $(1D)$ from the centerline to visualize only one side of the vortex street. The Reynolds number based on the wire diameter was too small to have any effect on the main flow. On the wire, a thin layer of paraffin oil was applied by hand which splits into very fine droplets. Electrical current was passed through the wire and the droplets vaporized to produce smoke which formed the patterns. The plane of the vortex street was illuminated by a lighting system which is a rectangular aluminium box with a reflector at the back, a 1000 watt halogen tube inside, and a narrow slit in the front which produced light sheet (for more details on lighting system see Ref. 14). The floor and the side walls of the tunnel were covered with black paper for better contrast. For visualizing the side view of the vortex street the smoke wire was placed perpendicular to the cylinder. The vortical patterns were photographed using a Nikon F3 camera.

3. RESULTS AND DISCUSSIONS

3.1 Near wake structure behind linearly tapered cylinders.

To examine the near wake structure, velocity signal from the hot-wire probe was collected and analyzed using a HP spectrum analyzer. The hot-wire probe, which was placed $2d_m$ behind the cylinder and offset $1d_m$ from the centerline of the model, was traversed from larger diameter end towards smaller diameter end at steps of $3\,mm$. At each spanwise location, both time series and its spectrum data were collected and stored in a disk for final analysis. First, the overall flow is discussed including the behaviour of hot wire signal along the span and effect of taper and Reynolds number on wake structure, followed by flow visualization results. To appreciate the effect of taper on wake structure, comparison of shedding geometry between tapered and straight cylinder is also presented. Comparisons with similar experiments are made, and conclusions are drawn.

It was observed during the experiment that the flow was significantly unsteady near the ends (within $5\,mm$ from end plate) of the cylinder. This was attributed to the horse-shoe vortices which are very unsteady. As the probe was traversed spanwise along Z-axis, it was observed that the signal from the hot-wire suddenly started becoming highly modulated implying the presence of two frequencies. Traversing further spanwise, the probe entered into a region where hot-wire signal showed no modulation indicating single frequency region of a cell. This change in hot-wire signal was also clear from the spectrum. Spectrum of the modulated signal had two distinct frequencies corresponding to the two adjacent cells. Typical results of this survey for 60:1 taper ratio cylinder are shown in figures 5 to 7. The hot-wire trace and its spectrum, at $Z = 9.9\,cm$, are shown in figure 5. The single dominant frequency at this spanwise location is $19.5\,Hz$. At $Z = 13.1\,cm$, the single dominant frequency is $23\,Hz$ as is evident from figure 7.

This implies that these two locations are in two different cells. Results as shown in figure 6 is for the location, $Z = 11.4\,cm$, which is in the boundary between two cells. Here two dominant peaks corresponding to two dominant frequencies of the adjacent cells are clearly visible. The sum, difference, and harmonics of these two frequencies are also present in the spectrum.

To estimate the cell length, it was conveniently defined as the distance from very highly modulated time series location to next very highly modulated time series location. It was observed that highly modulated region was fairly broad implying that the boundary between two cells was like a band. The band width was different at each boundary and varied from $2d_m$ to $4d_m$. The mid point of this band was chosen as the convenient boundary between two cells. The cell lengths were determined for all the four cylinders and the results plotted in figure 8. It is evident from the figure that more cell boundary points are created as the taper is increased, i.e. taper ratio is decreased.

The variation in number of cells with taper ratio was investigated to study the effect of three dimensionality on cellular structure in the flow behind the cylinders. The results are plotted in figure 9. It is clear from the figure that number of cells decrease with increasing taper ratio. It also appears that number of cells reach an asymptotic value. The data of Piccirillo and Van Atta are also included on the same figure for comparison. Good agreement is observed between the data sets.

The effect of Reynolds number on the number of cells and the Strouhal number-Reynolds number relationship for tapered cylinders were also investigated. The Strouhal and Reynolds numbers were calculated based on cell mid point diameter and its frequency at fixed centerspan Reynolds number. The results are plotted in figures 10 and 11. The data of Piccirillo and Van Atta [8] are also included in the figures for comparison. Figure 10 shows the variation in the number of cells with Reynolds number. It is clear from the figure that the number of cells increase with Reynolds number. Figure 11 shows the variation of Strouhal number with Reynolds number along with the Roshko's

curve [1] . It is clear from the figure that the data of the present experiments, for all taper ratios, are closer to Roshko's curve as opposed to the data points of Piccirillo and Van Atta [8]. This indicates that the Strouhal number - Reynolds number relationship is perhaps independent of taper ratio and closely follows Roshko's curve.

Flow visualization results for comparison of the vortex shedding geometry between tapered and straight cylinder are shown in figure 12. It is clear from the figure that in the case of the tapered cylinder shedding vortices are always oblique with vortex splits in several spanwise locations indicating the presence of cellular structure. However, in the case of the straight cylinder the shedding vortices, as shown in figure 12a, are either oblique or parallel depending on the end conditions but continuous with no vortex splits. A side view of the vortex structure in the wake behind the straight cylinder is also shown in the same figure. The Karman Vortex street is clearly observed in this picture.

Figure 13 shows flow visualization pictures for different taper ratio models at a fixed centerspan Reynolds number of 120. Vortex splitting, as observed in these figures, occurs at the places where the kink appears in the shed vortex lines and these locations are marked with an arrow. The two parts of the split vortex are not very clear in the photographs as the vortex street was illuminated in a plane. An increasing taper, i.e. decreasing taper ratio appears to split the vortex line in more spanwise locations implying creation of more cells.

3.2 Control of obliqueness of vortices shed behind straight and linearly tapered cylinder.

The control of obliqueness of vortices is first studied for straight cylinder and then for tapered cylinder. The effective length of the straight cylinder i.e length between end plates is $150\,mm$. The pressure port is located at the base of the cylinder at one end near the end plate. The cylinder is pulled from one side in steps to measure the base pressure at various spanwise locations. The base pressure is measured for parallel and oblique vortex shedding geometries behind straight cylinder. A control technique is developed to alter the base pressure for obtaining parallel and oblique vortex shedding behind straight cylinder. The base pressure is also measured for tapered cylinder and the data is correlated with the straight cylinder case.

3.2.1 Control of obliqueness of vortices shed behind straight cylinder

To study the control of obliqueness of vortices shed behind straight cylinder, first oblique vortices were created by giving a slight angle of attack to the end plate. Flow visualization picture in figure 14(a) shows the vortex shedding geometry without any control cylinder. It is clear from the picture that the vortices are oblique. The base pressure distribution corresponding to this shedding geometry is shown in figure 14(b). It seems from the figure that the pressure coefficient, C_p, is higher towards the spanwise location, where the shed vortex element travels less distance downstream. Qualitatively this geometry also follows from the fact that a spanwise base flow is induced from high pressure side to low pressure side which causes the vortex element to travel less distance downstream near the high pressure side. The base pressure continuously decreases towards the other end where vortex element travels greater distance downstream.

To alter the base pressure for obtaining parallel shedding, a control cylinder ($D/d = 3$) was placed vertically towards the high pressure side upstream of the test cylinder. Its spanwise location was fixed at $Z/d = 69$, while the X-location was varied to obtain parallel shedding. A typical result is shown in figures 15,16 and 17. Figure

15 shows the results when the control cylinder is located at $X/d = 9.3$. Figure 15(a) shows the vortex shedding geometry. The vortex shedding geometry is clearly oblique with vortex element travelling greater distance downstream near the $Z = 0$ end as compared to the other end. Base pressure distribution corresponding to this geometry is shown in figure 15(b). Base pressure distribution shows that pressure near the region of control cylinder location is greater than the pressure near the farther end plate. Thus a spanwise base flow is induced from the $Z = 75$ end to $Z = 0$ end. To alter the base pressure and hence stop the base flow the control cylinder was moved downstream. Figure 16 shows the results with control cylinder at $X/d = 6$. Figure 16(a) shows the flow visualization result. It is clear from the figure that vortex shedding is parallel. Base pressure distribution corresponding to parallel shedding geometry is shown in figure 16(b). It is clear that the base pressure shows a sudden dip near the spanwise location of control cylinder, while it is constant over the major part of the span except near the end plates, which is due to the end plate boundary layers. Control cylinder was moved slightly downstream at $X/D = 4.1$ to look at the change in vortex shedding geometry. Corresponding vortex shedding geometry and base pressure distribution are shown in figure 17. Figure 17(a) shows that the shedding is oblique with vortex element travelling greater distance downstream near the control cylinder location end as compared to the $Z = 0$ end. This shows that for a given spanwise location of control cylinder there is a fixed upstream location where it should be placed to induce parallel shedding. The optimal locations,i.e locations for inducing parallel shedding were thus determined for various spanwise locations from $Z/d = 55$ to $Z/d = 75$. To study the effect of control cylinder diameter on their optimal locations, these locations were determined for control cylinders of $5\,mm$ and $8\,mm$ diameter. The study was conducted in the spanwise region $Z/d = 55$ to $Z/d = 75$. The results are plotted in figure 18. It is clear from the figure that for a given control cylinder, its optimal location moves away from the cylinder as it moves towards the end plate. Also, at a fixed spanwise

location, the optimal location moves further upstream as the control cylinder diameter is increased. This graph can also serve to predict approximately the optimal location of control cylinder of given diameter.

3.2.2 Control of obliqueness of vortices shed behind tapered cylinder

The same control technique was tried to control the oblique vortex shedding behind tapered a linearly tapered cylinder. From the study on straight cylinders it is clear that the base pressure is responsible for oblique vortex shedding, so the base pressure was measured behind tapered cylinder of taper ratio 150:1 at Reynolds numbers 80, 120 and 150. The results are shown in figures 19, 20 and 21 for the three Reynolds numbers. Base pressure distributions in these three figures show that pressure is lower towards the spanwise region where vortex element travels more distance downstream. This result is similar to the straight cylinder result in figure 14. This implies that the same mechanism of spanwise base flow from high base pressure side to low base pressure side is responsible for oblique shedding behind a tapered cylinder. So the same technique of using control cylinder was applied to control the obliqueness in shed vortices behind tapered cylinders. Here only flow visualization study was conducted and the results are presented in figure 22 (a,b). It is clear that parallel shedding over the entire span is not achieved but the control over the obliqueness near the spanwise location of control cylinder is possible. This is because of the cellular nature of the wake.

4. CONCLUSIONS AND SCOPE OF FUTURE WORK

4.1 Conclusions

This experiment studied the effect of taper on the near wake structure behind linearly tapered cylinders. The mechanism behind the oblique vortex shedding was also studied. The primary effect of taper is to produce cellular structures in the wake. The effect of increasing taper ratio is to decrease the number of cells. As the taper ratio is increased further the number of cells seem to reach an asymptotic value. The boundary between two cells is fairly broad instead of a sharp transition. In the present study, the width of the boundary was found to vary from $2d_m$ to $4d_m$. Flow visualization showed vortex splitting at various spanwise locations which were in the boundary of two cells as obtained from the hot wire results. The effect of Reynolds number was to increase the number of cells for a given tapered cylinder. The Strouhal number - Reynolds number relationship, which was found to be independent of taper ratio, closely follows the Roshko's curve.

A simple control technique of placing a vertical control cylinder towards one side of test cylinder to control the shedding geometry behind straight cylinder is developed. The pressure data taken at the base of the cylinder, shows that symmetric base pressure [13] is not the only factor responsible for parallel shedding but a constant base pressure over major part of span can also induce parallel shedding. The optimal location of the control cylinder moves upstream as its diameter is increased at the fixed spanwise location. An experimental plot is obtained to predict approximately the location of control cylinder of given diameter for inducing parallel shedding. The same control technique when applied to tapered cylinder shows that it is not possible to induce parallel shedding over the entire span because of the cellular structure of the wake but the oblique angle can be reduced to some extent near the spanwise location of the control rod.

4.2 Scope for future work

The present study has answered some interesting questions. However, it raise some others that are worth pursuing. Having investigated the near wake structures, it would be interesting to investigate how the cellular structures interact with each other and how the boundary of the two cells behave further downstream i.e whether the cells merge with each other or new ones are created. Another important aspect to investigate here would be the flow field across the wake at the cell boundaries both with the help of flow visualization and quantitative measurements. This would give more insight into the understanding of the vortex splitting process which connects one cell to the other.

REFERENCES

1. Roshko, A. (1954) "On the development of turbulent wakes from vortex streets," NACA Rep. 1191.
2. Gaster, M. (1969) "Vortex shedding from slender cones at low Reynolds number," J. Fluid Mech., Vol. 38, pp. 565–576.
3. Gaster, M. (1971) "Vortex shedding from circular cylinders at low Reynolds numbers," J. Fluid Mech., Vol. 46, pp. 749–756.
4. Van Atta, C. W. & Piccirillo, P. (1990) "Topological defects in vortex streets behind tapered circular cylinders at low Reynolds numbers," In "New Trends in Nonlinear Dynamics and Pattern Phenomenon: The Geometry of Non Equilibrium" ed. by P. Coullet & P. Huerre, pp. 243–250, Plenum.
5. Lewis, C. G. & Gharib, M. (1992) "An exploration of wake three dimensionalities caused by a local discontinuity in cylinder diameter," Phys. Fluids A4, pp. 104–117.
6. Noak, B. R., Ohle, F. & Eckelmann, H. (1991) "On cell formation in vortex streets," J. Fluid Mech., Vol. 227, pp. 293–308.
7. Gerich, D. & Eckelmann, H. (1982) "Influence of end plates on the shedding of circular cylinders," J. Fluid Mech., Vol. 122, pp. 109–121.
8. Piccirillo, P. & Van Atta, C. W. (1993) "An experimental study of vortex shedding behind linearly tapered cylinders at low Reynolds number," J. Fluid Mech., Vol. 246, pp. 163–195.
9. Tritton, D.J. (1959) "Experiments on the flow past a circular cylinder at low Reynolds numbers," J. Fluid Mech., Vol. 174, pp. 173.
10. Ramberg, S.E. (1983) "The effects of yaw and finite length upon upon the vortex wakes of stationary and vibrating circular cylinders. " J. Fluid Mech., Vol.128, 81.

11. Williamson, C.H.K. (1988) "Defining a universal and continuous Strouhal - Reynolds number relationship for the laminar vortex shedding of a circular cylinder." Phys. Fluids 31, 2742.

12. Eisenlohr, H., and Eckelmann, H. (1989) "Vortex splitting and its consequences in the vortex street wake of cylinders at low Reynolds numbers." Phys. Fluids A1, 189.

13. Hammache, M., and Gharib, M. (1991) "An experimental study of the parallel and oblique vortex shedding from circular cylinders." J. Fluid Mech., Vol 232, pp. 567–590.

14. Dua, M.S. & Nundlall, R (1995) "An experimental study of the vortical flow over a delta wing at high angles of attack," B.Tech. project report, Dept. of Aerospace Engineering, I.I.T Kanpur.

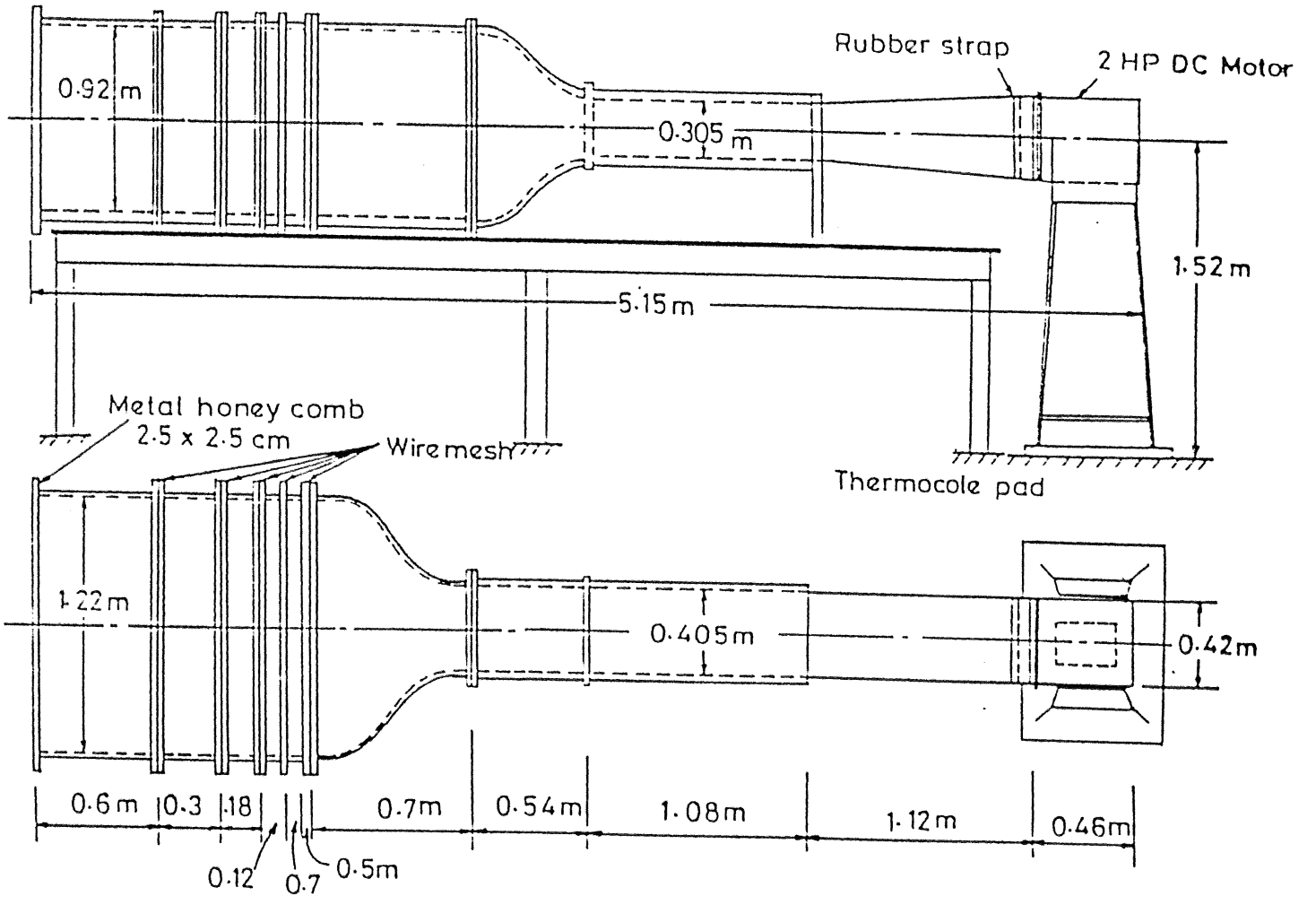

FIGURE 1. Wind Tunnel layout.

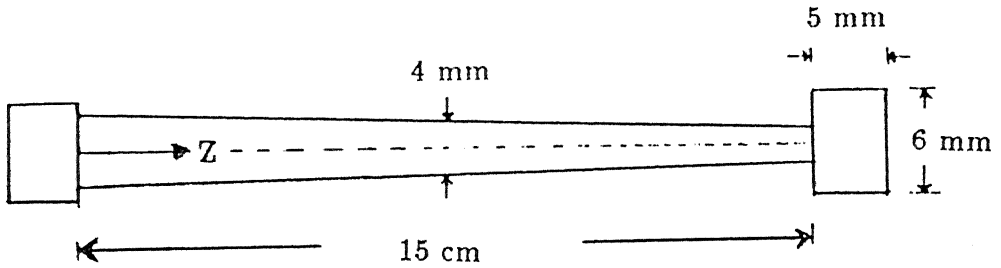

FIGURE 2. A typical model geometry.

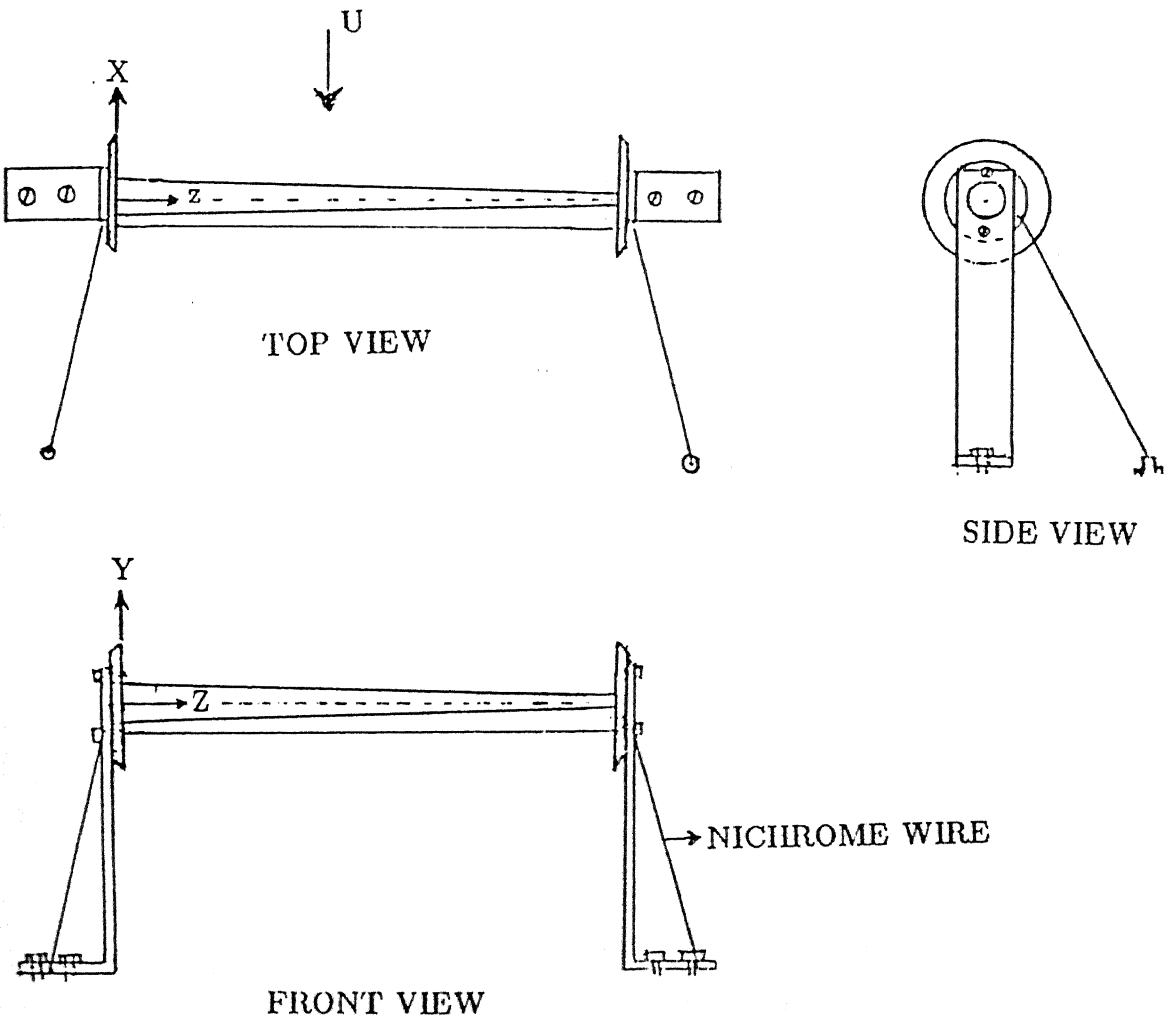

FIGURE 3. Experimental set up (not to scale).

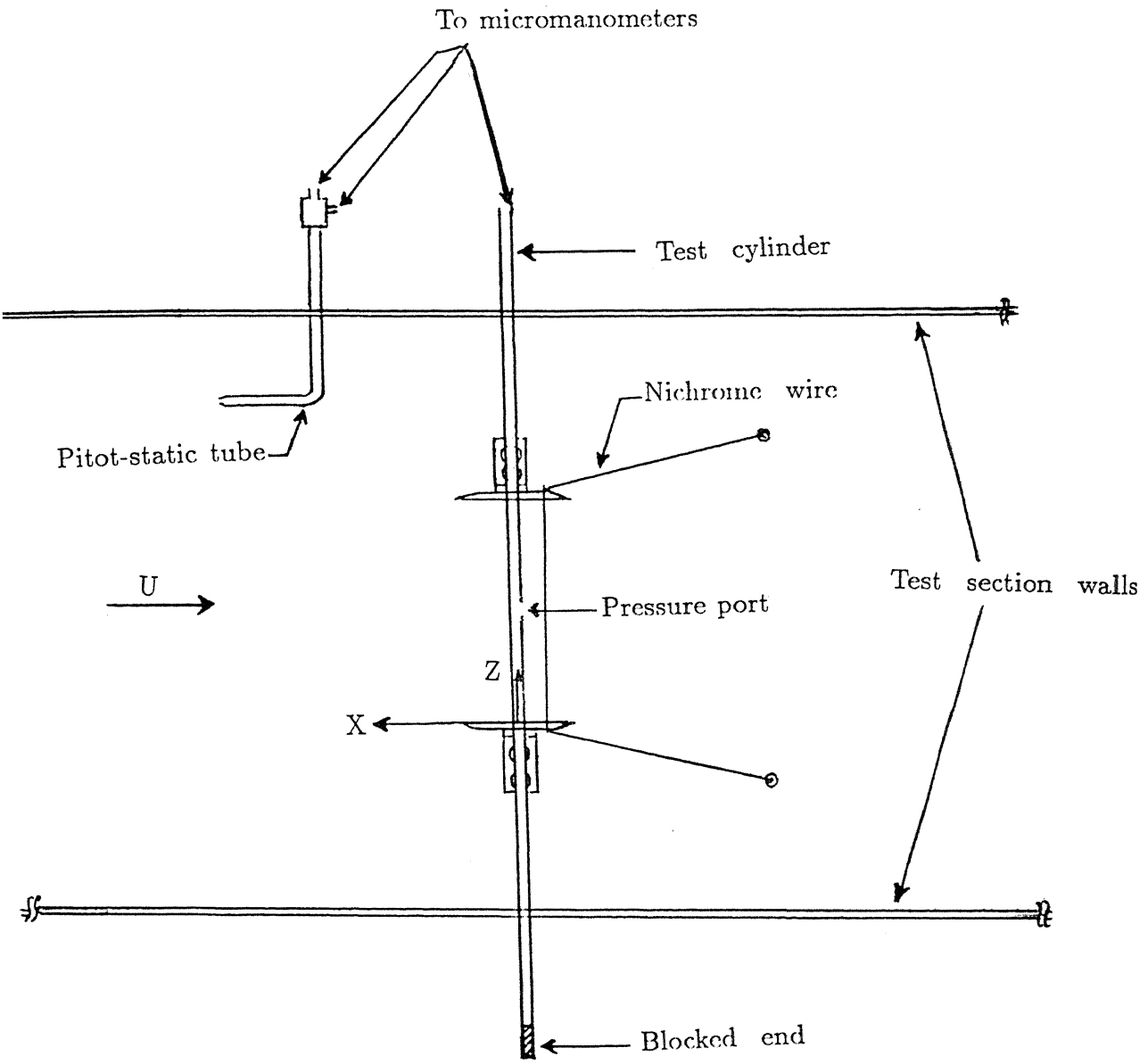

FIGURE 4. Schematic of the experimental set up for straight cylinder with axes convention shown (not to scale).

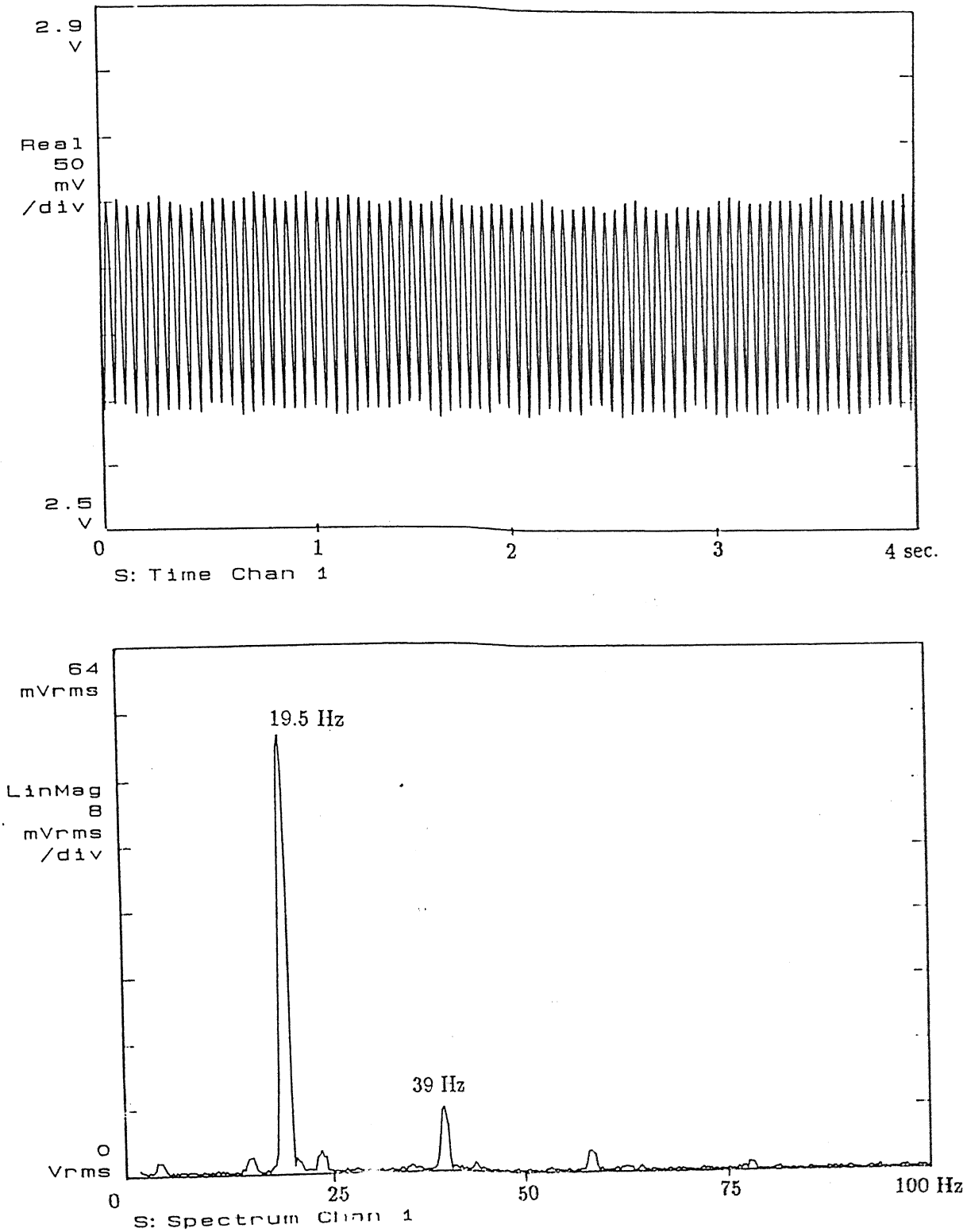

FIGURE 5. Time series and its spectrum at $Z = 9.9$ *cm.* for taper ratio 60.

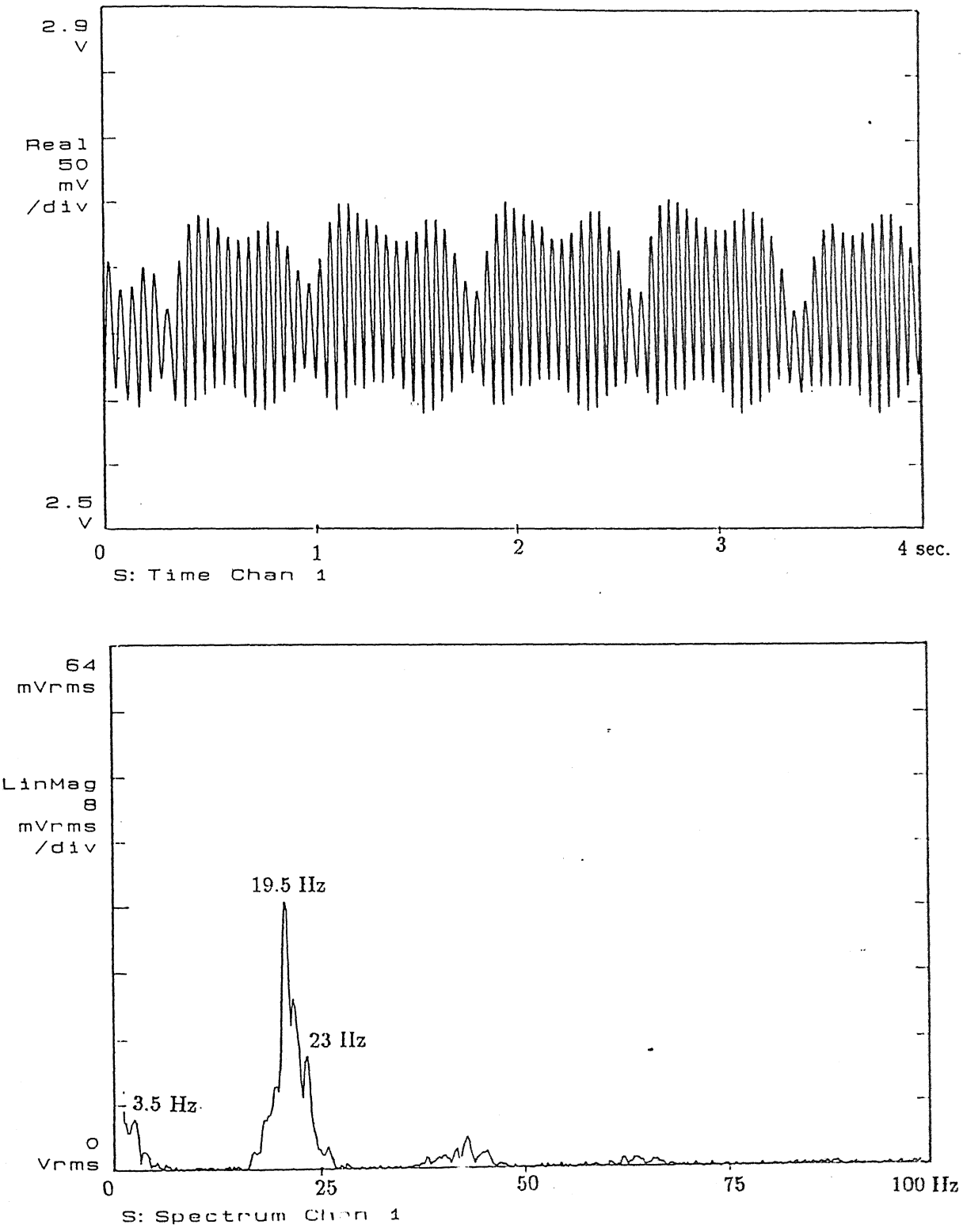

FIGURE 6. Time series and its spectrum at $Z = 11.4\ cm.$ for taper ratio 60.

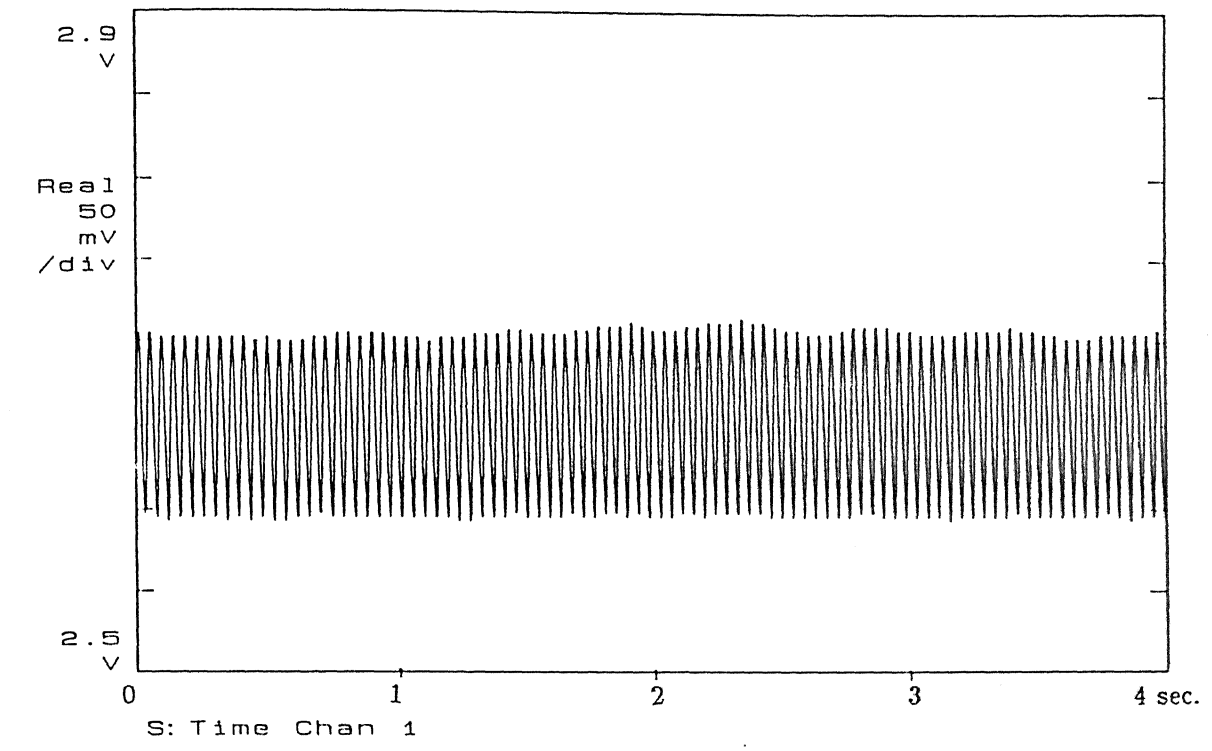

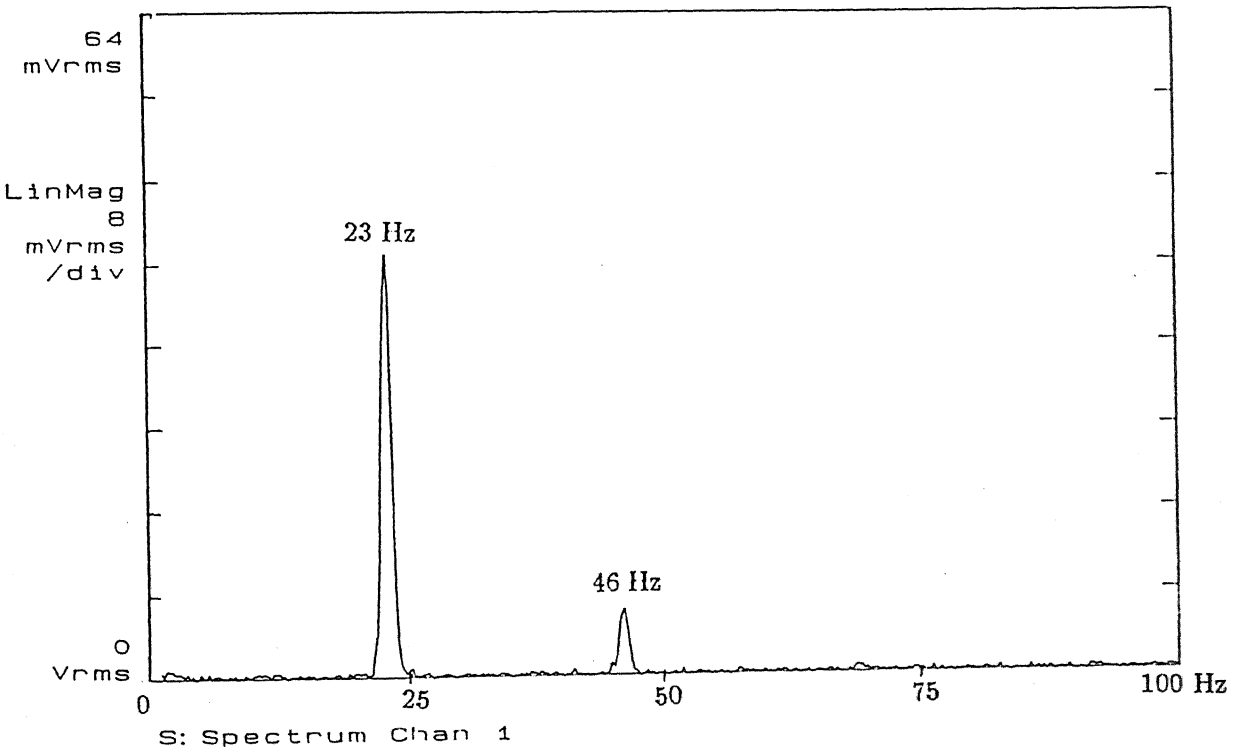

FIGURE 7. Time series and its spectrum at $Z = 13.1\ cm.$ for taper ratio 60.

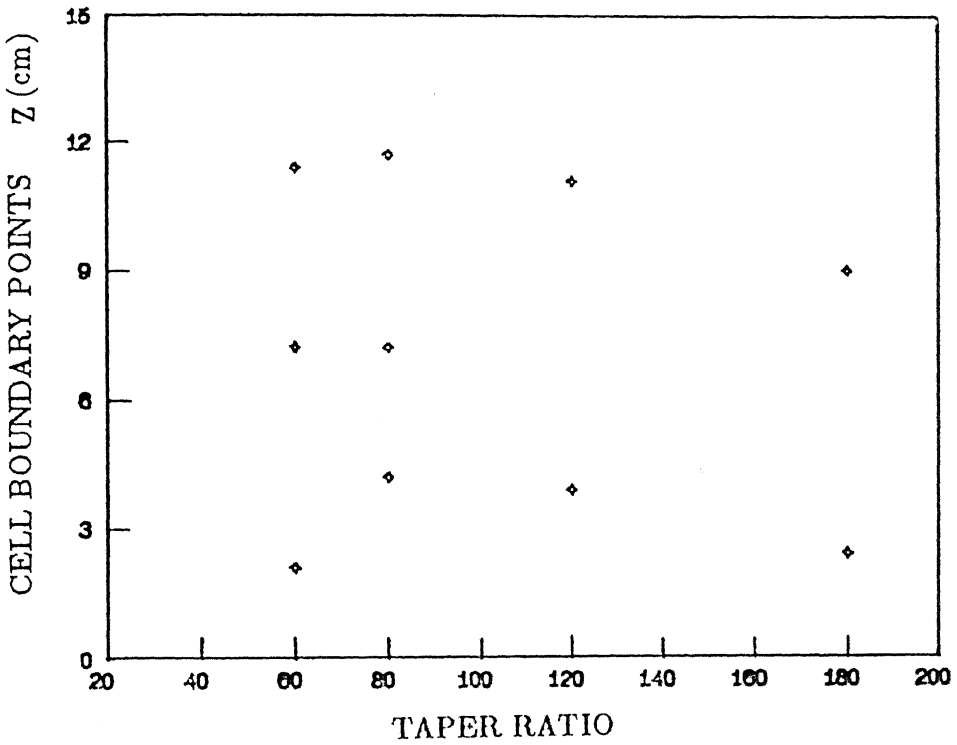

FIGURE 8. Cell boundary point locations for tapered cylinders at $Re_{cs} = 120$.

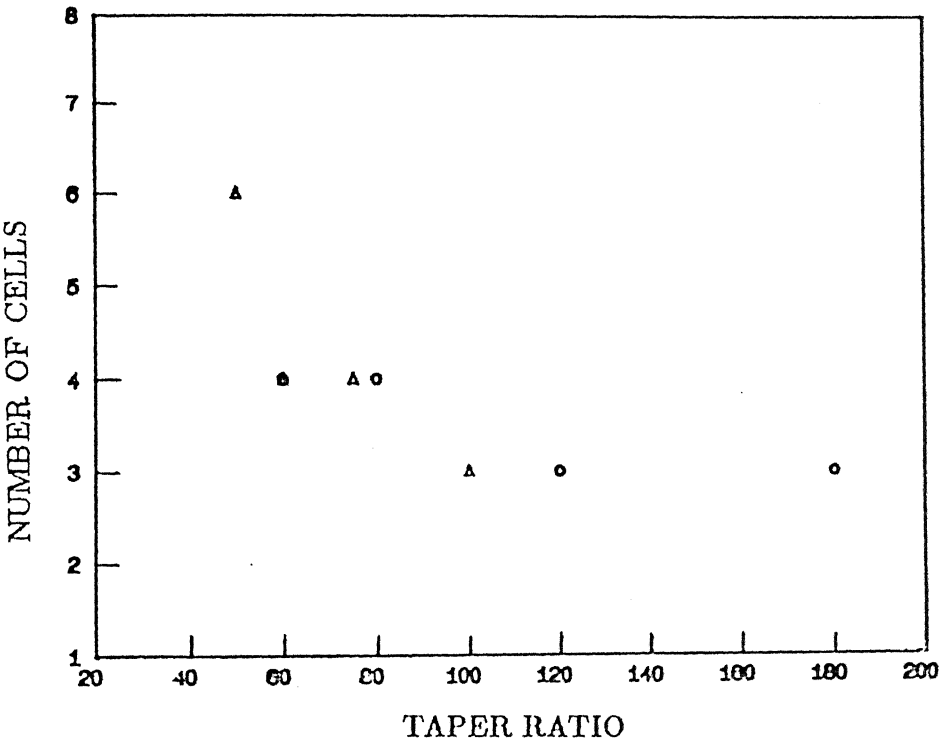

FIGURE 9. Number of shedding cells for all cylinders plotted against taper ratio at $Re_{cs} = 120$. △, Piccirillo & Van Atta (1993); ○, present experiment.

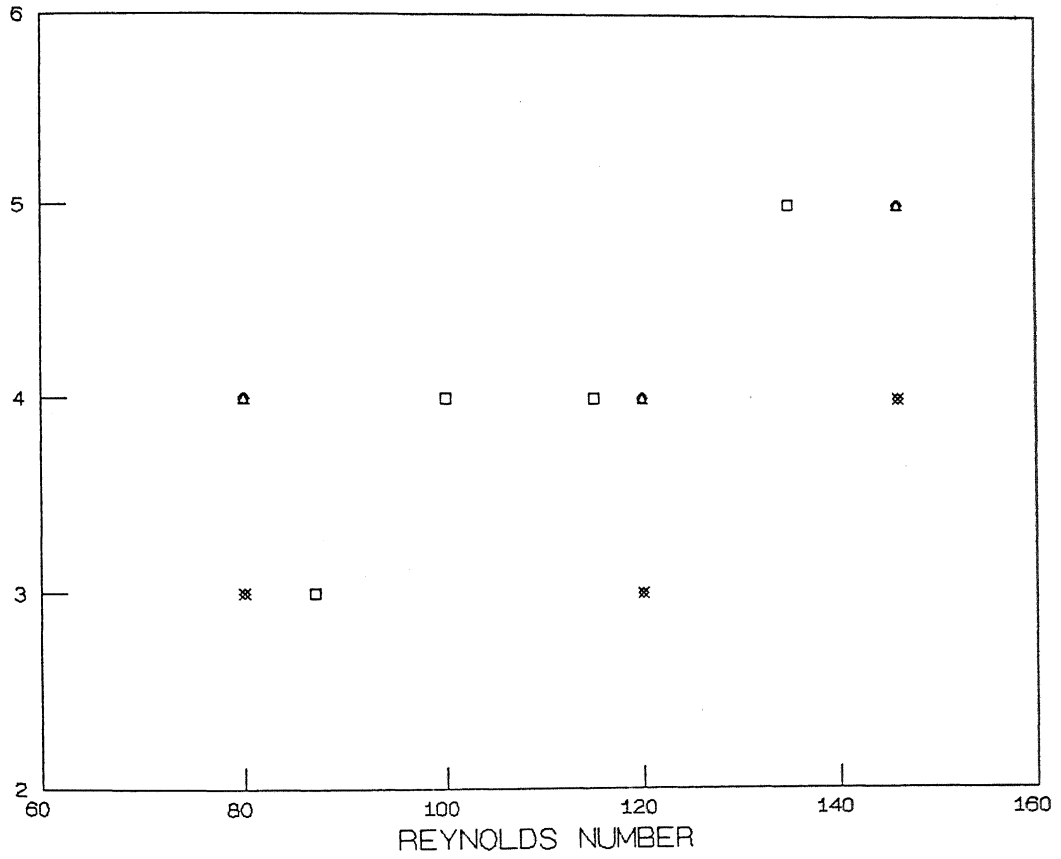

FIGURE 10. Number of shedding cells plotted against centerspan Reynolds number. ○, 60 : 1 cylinder; △, 80 : 1; ◇, 120 : 1; ×, 180 : 1; □, data of Van Atta *et al.*

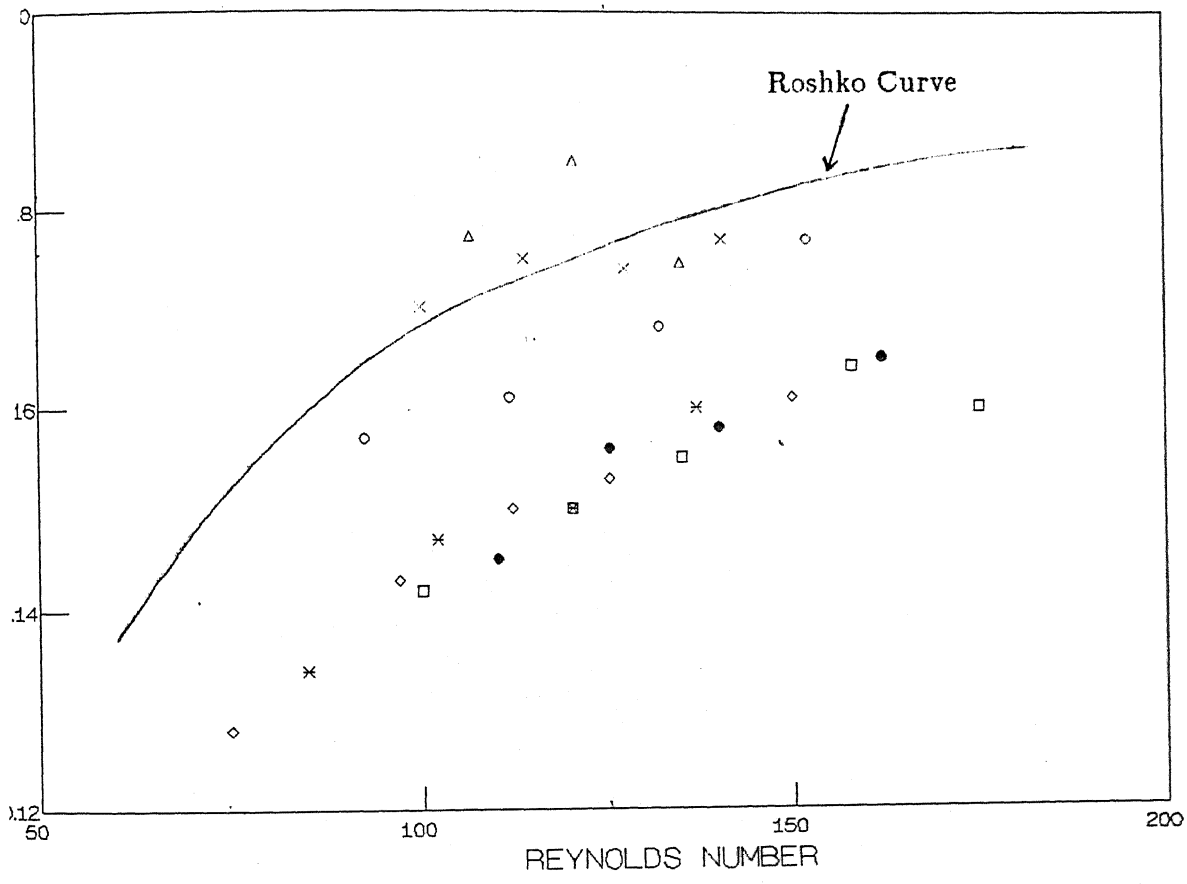

FIGURE 11. Cell Strouhal number plotted against cell mid point Reynolds number: ○, 60 : 1, $Re_{cs} = 120$; ×, 80:1, $Re_{cs} = 120$; △, 120:1, $Re_{cs} = 120$; ◇, ×, □, •, data of Piccirillo *et al.* □, 60:1, $Re_{cs} = 135$; ◇, 75 : 1, $Re_{cs} = 102$; ×, 60:1, $Re_{cs} = 115$; •, 75:1, $Re_{cs} = 139$. Re_{cs} is the centerspan Reynolds number.

a)

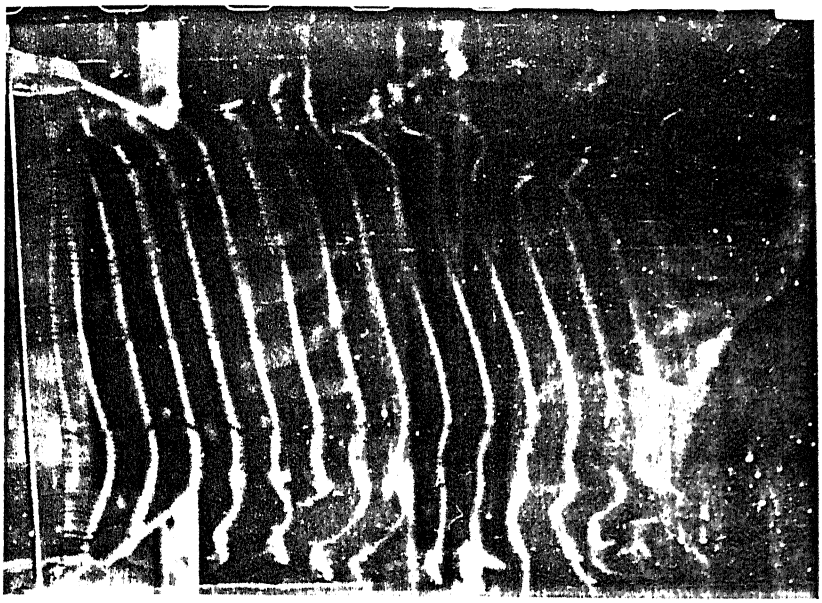

b)

Figure 12(a,b). For caption see next page.

c)

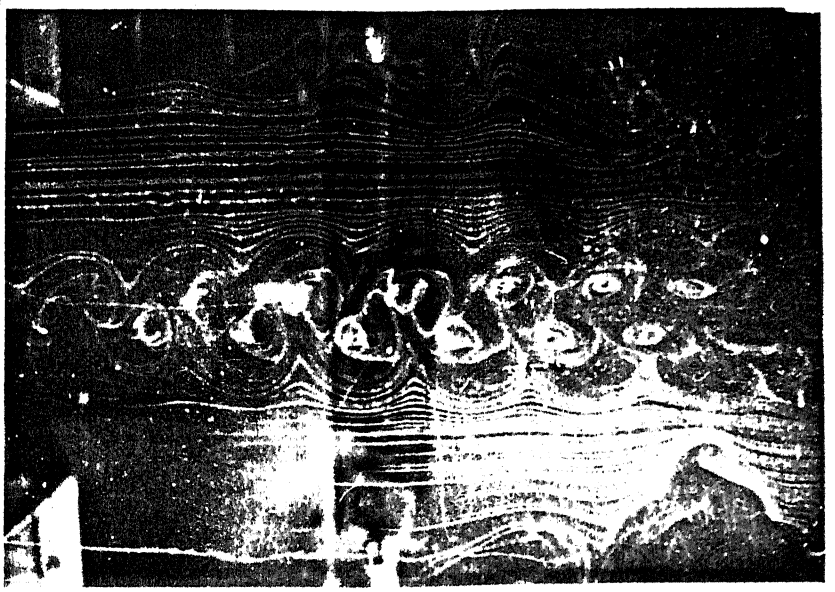

FIGURE 12. Typical comparison of vortex shedding geometry behind tapered and straight cylinder. (a) straight cylinder, (b) tapered cylinder, and (c) side view of the vortex pattern (i.e. Vortex street) behind a straight cylinder.

a)

b)

Figure 13(a,b). For caption see next page.

a)

b)

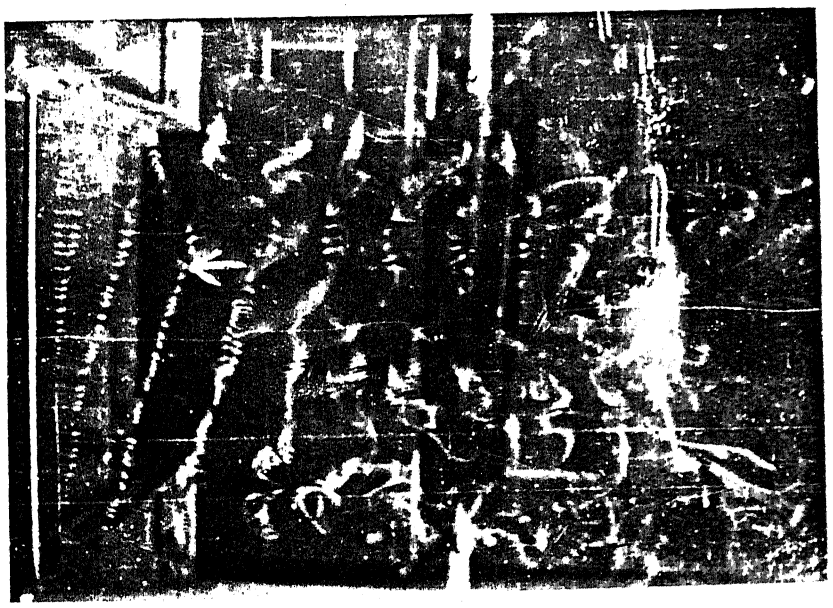

FIGURE 13. Flow visualization pictures for models with taper ratios of a) 60 : 1, b) 80 : 1, c) 120 : 1, and d) 180 : 1. In all the pictures the flow direction is from left to right. Arrows indicate the locations of vortex splitting.

a)

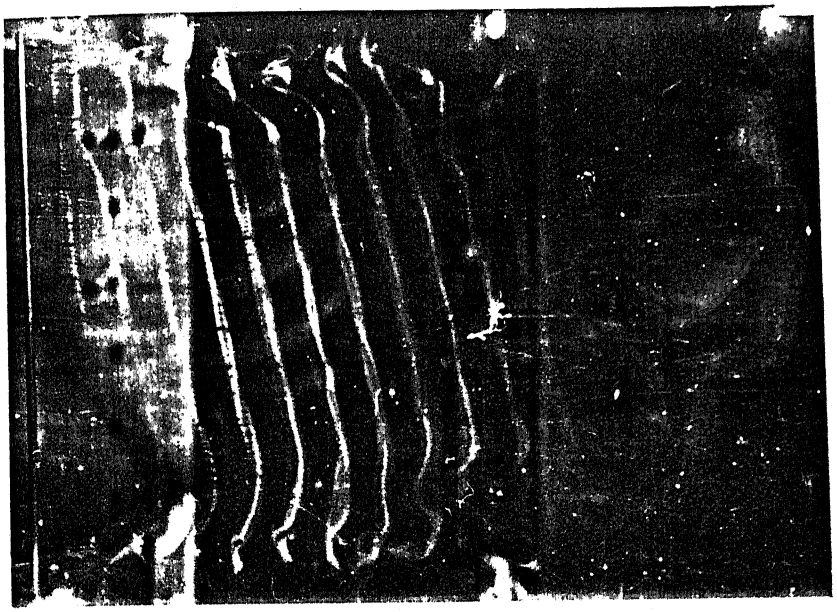

b)

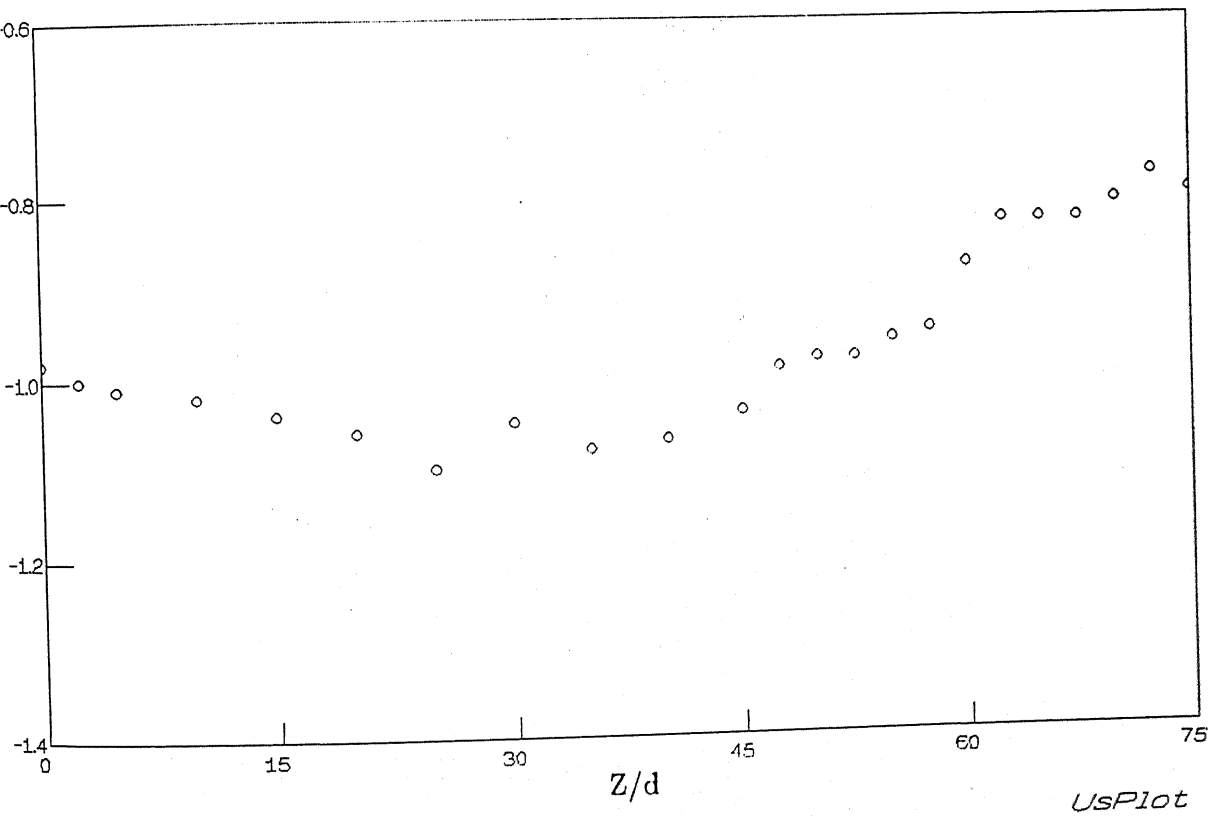

FIGURE 14. Oblique vortex shedding behind straight cylinder without any control cylinder. a) Flow visualization b) Base pressure distribution.

a)

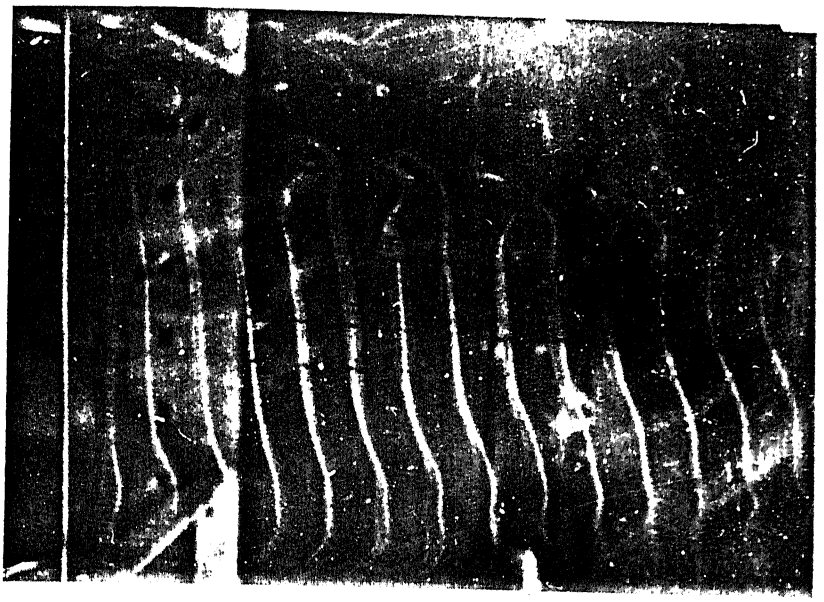

b)

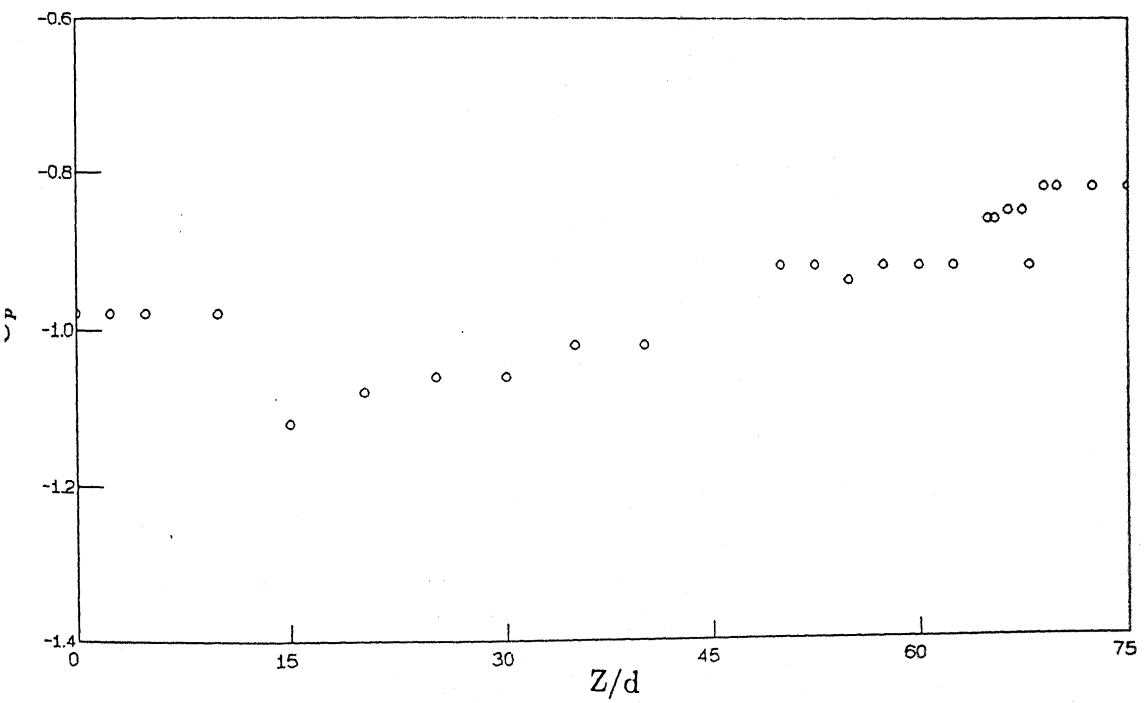

FIGURE 15. Vortex shedding geometry and base pressure distribution with control cylinder($D/d = 3$) at $Z/d = 69$ and $X/d = 9.3$.

a)

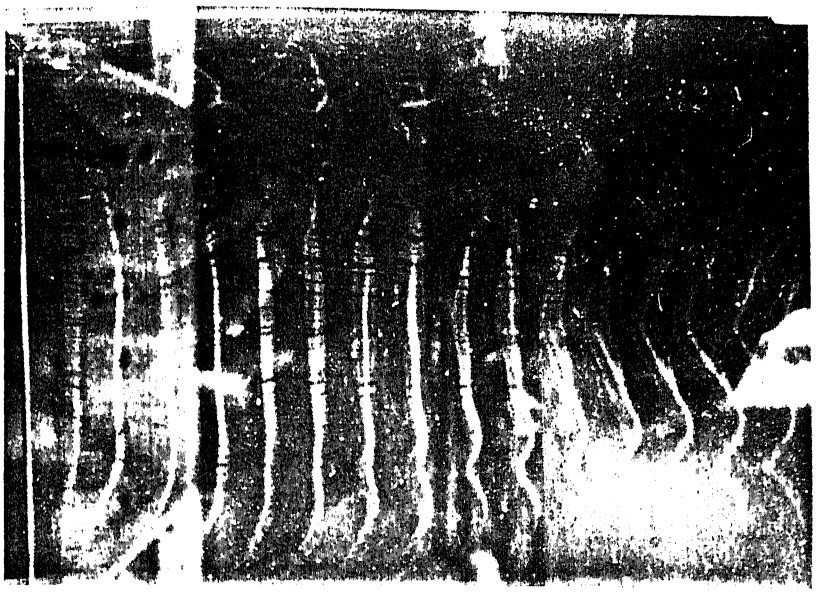

b)

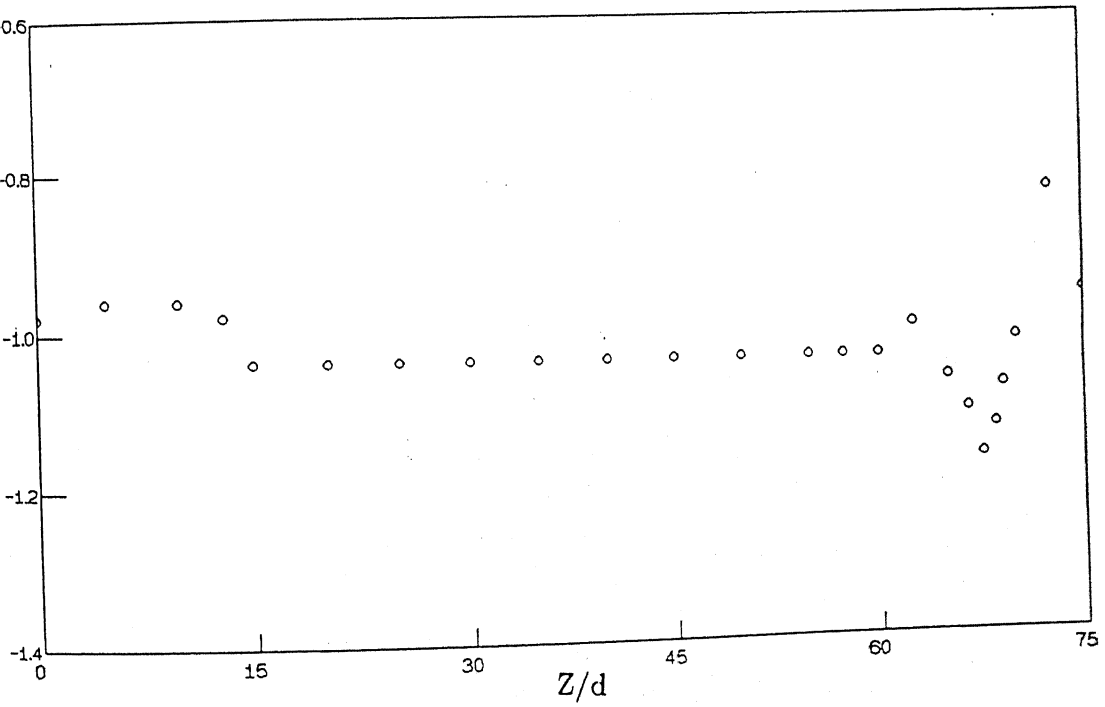

IGURE 16. Parallel shedding induced by a control cylinder($D/d = 3$) at optimal location of $Z/d = 69$ and $X/d = 6$. a) Flow visualization b) Base pressure distribution.

a)

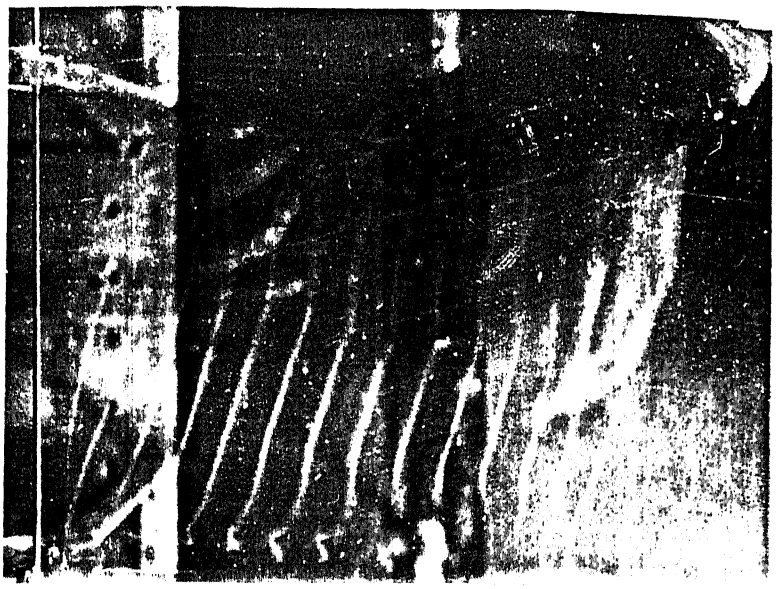

b)

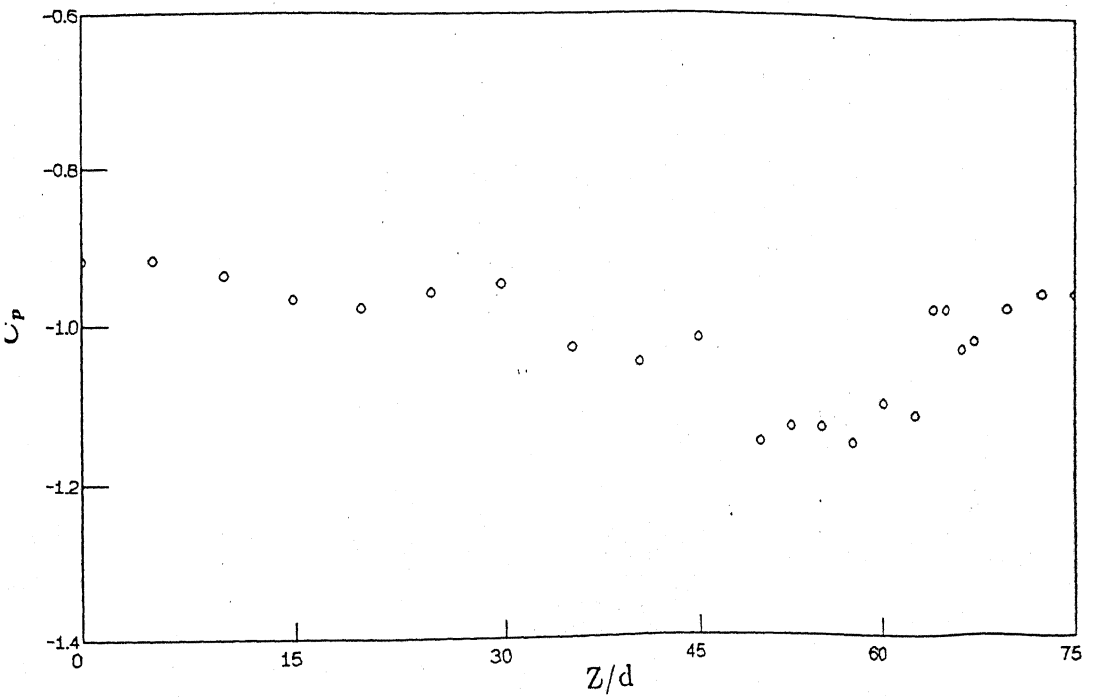

FIGURE 17. Vortex shedding geometry and base pressure distribution with control cylinder($D/d = 3$) at $Z/d = 69$ and $X/d = 4.1$.

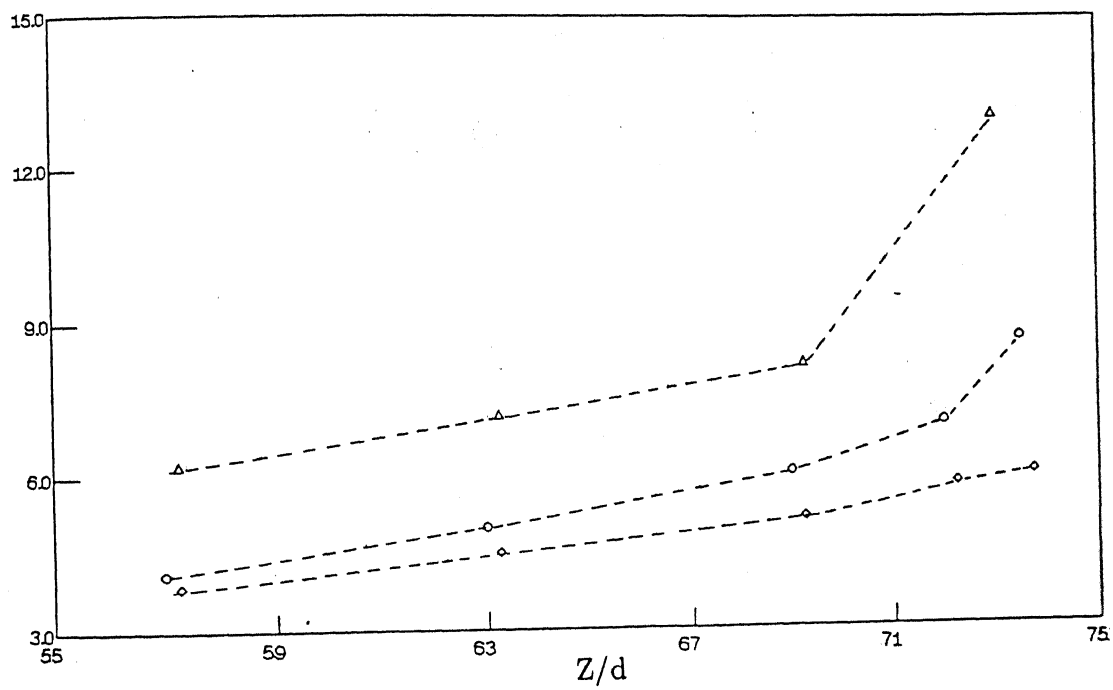

FIGURE 18. Variation of 'control cylinder location for inducing parallel shedding' along the span for various control cylinder diameters. $\triangle$, $D/d = 4$; $\bigcirc$, $D/d = 3$; $\diamond$, $D/d = 2.5$.

a)

b)

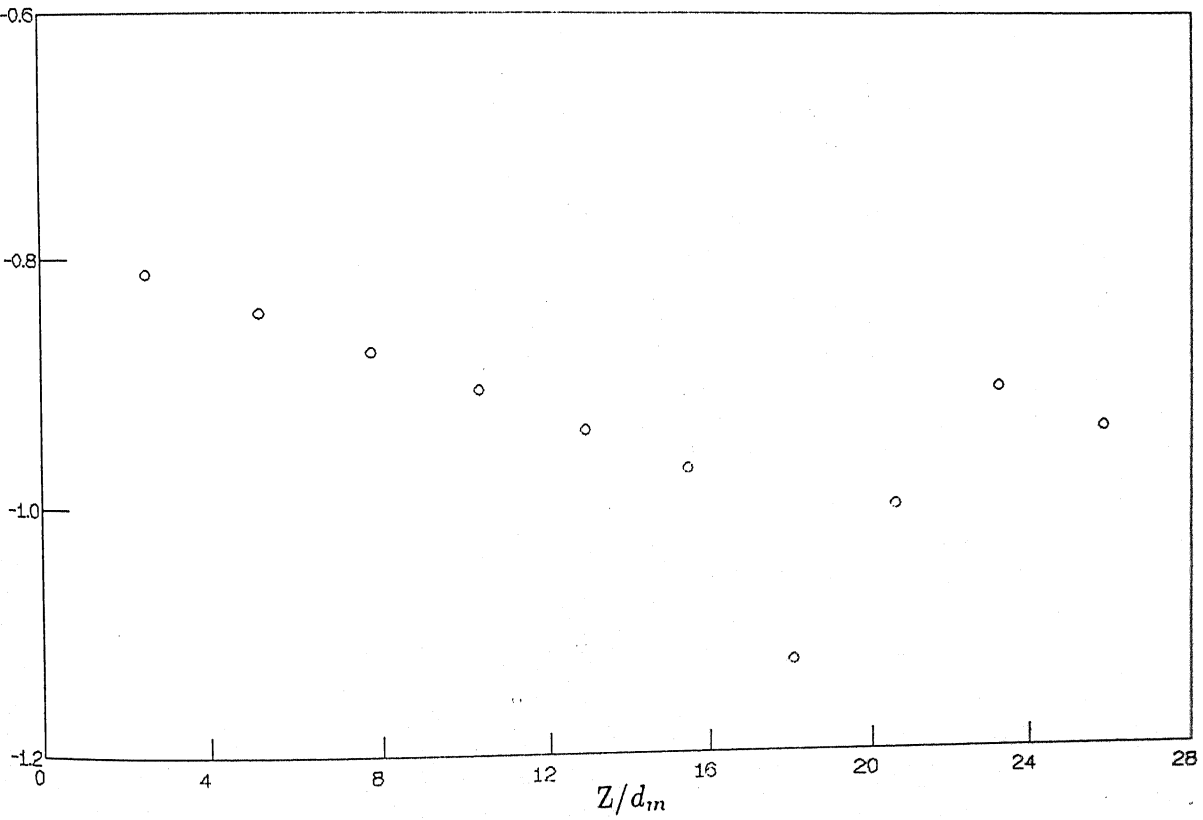

FIGURE 19. Vortex shedding geometry and base pressure distribution on tapered cylinder of taper ratio 150 at $Re_{cs} = 80$.

a)

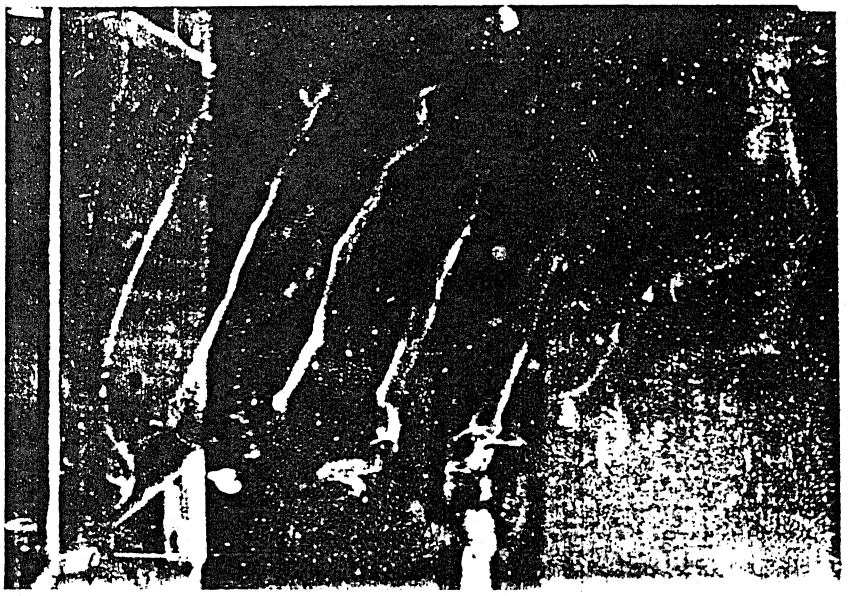

b)

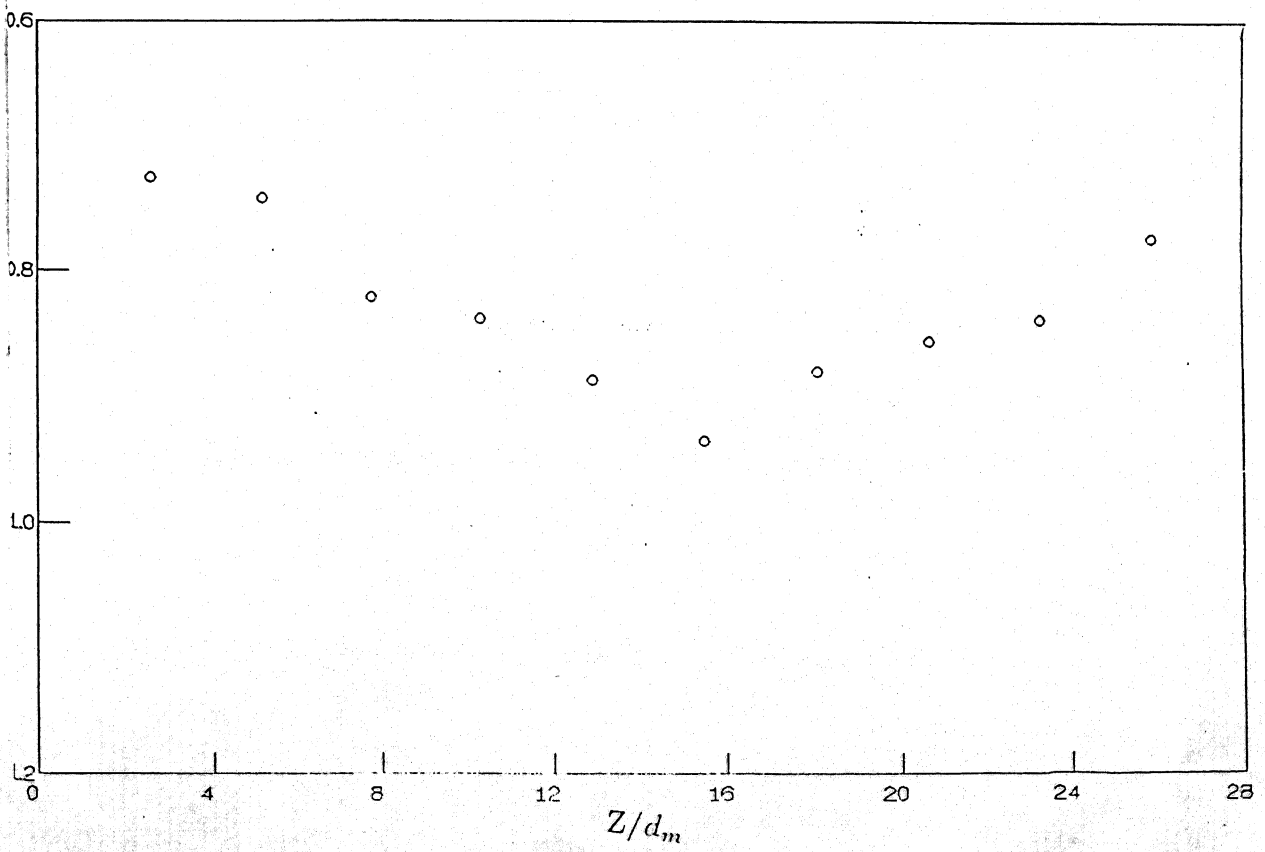

FIGURE 20. Vortex shedding geometry and base pressure distribution on tapered cylinder of taper ratio 150 at $Re_{cs} = 120$.

a)

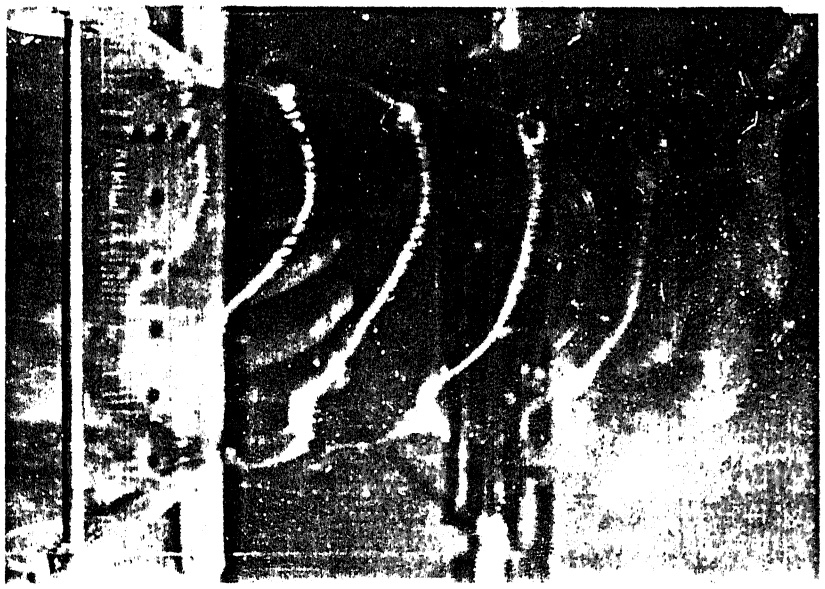

b)

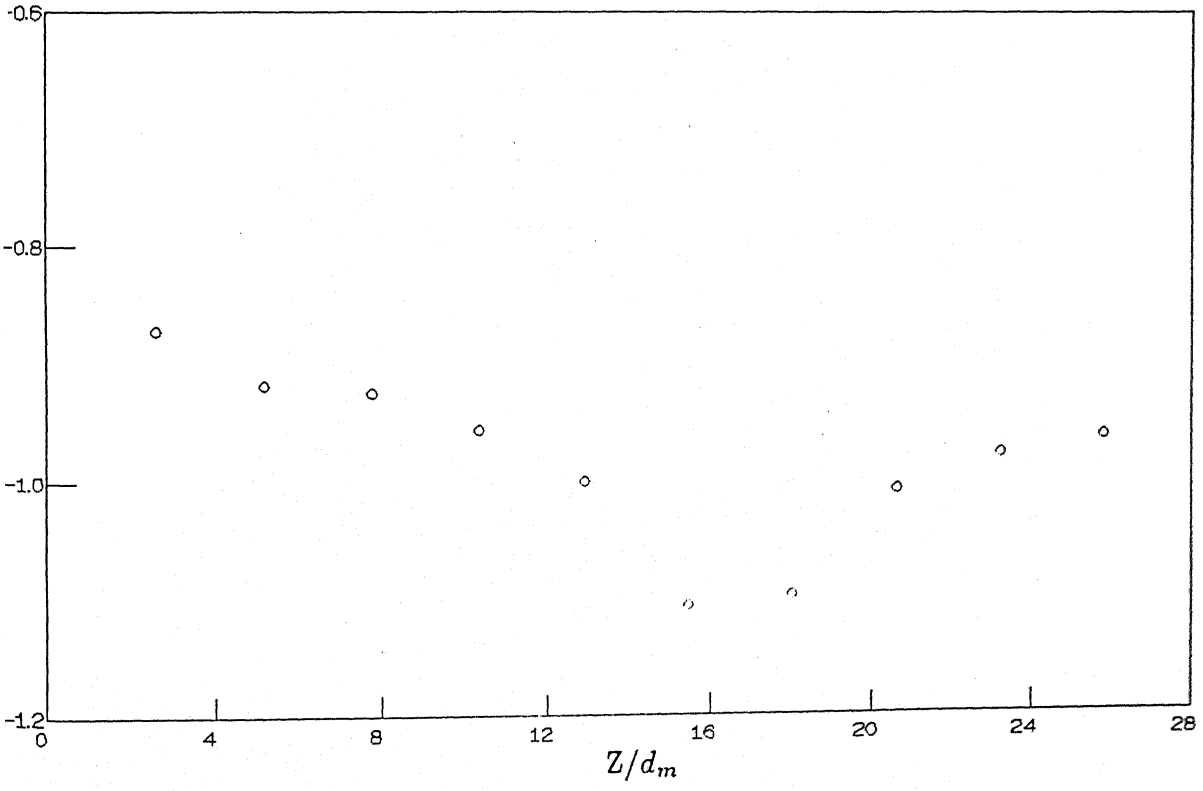

FIGURE 21. Vortex shedding geometry and base pressure distribution on tapered cylinder of taper ratio 150 at $Re_{cs} = 150$.

a)

b)

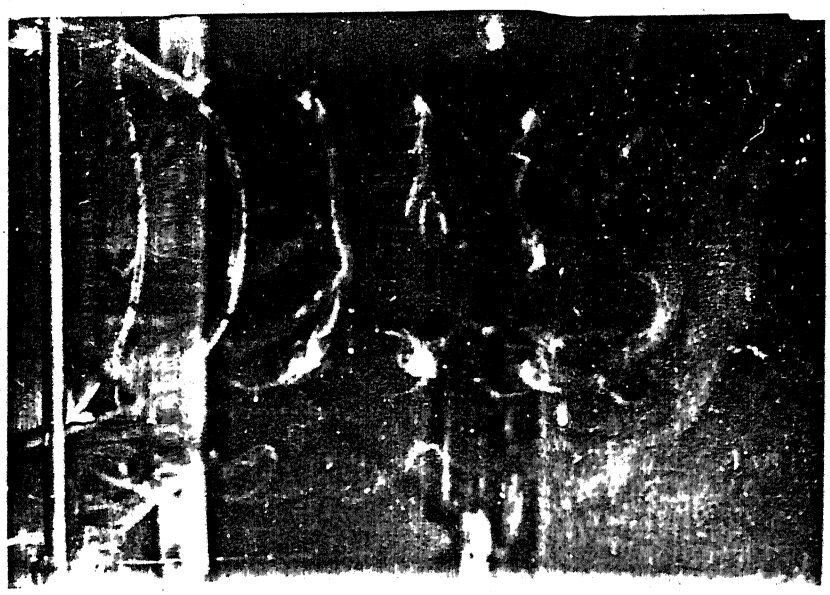

URE 22. Control cylinder technique applied to tapered cylinder of taper ratio 150 : 1 at $Re_{cs} = 120$. a) Vortex shedding geometry without control cylinder b) Vortex shedding geometry with control cylinder. Arrow shows the location of control cylinder.